Multi-Objective Design Optimization Using Nash Games

Jean-Antoine Désidéri and Régis Duvigneau

Opale Project-Team

INRIA, Sophia-Antipolis Méditerranée Centre

B.P. 93, 2004 Route des Lucioles, F-06905 Sophia Antipolis Cedex

France

Abderrahamane Habbal

Department of Mathematics, and Opale Project-Team

University Nice Sophia-Antipolis

06108 Nice Cedex 02

France

1 Multidisciplinary competition in complex design optimization - Nash games

In the engineering office, many of the optimization problems that are raised by designers of complex systems are by nature *multi-objective*. For instance, in aerodynamic shape optimization for the design of commercial airplanes, one focus is the lift maximization in the critical phase of take-off or landing, another is drag minimization in the cruise regime since it directly determines kerosene consumption or range, but other criteria are also important : those related to stability or maneuverability that are linked to aerodynamic moments, or those imposed by manufacturing constraints, etc. Evidently, the resulting multi-objective optimization problems are inevitably also *multipoint*, since they are associated with different flight regimes (different Mach and Reynolds numbers, and angles of attack) and configurations (e.g. possible deployment of special high-lift devices). Consequently, the accurate evaluation of such criteria by means of high-fidelity models requires the efficient simulation of several flowfields by the numerical approximation of the gas dynamics equations, typically by finite volumes. In addition, different couplings of aerodynamics with other physical phenomena are also of critical importance in the performance evaluation of a design : structural strain, stress and fatigue, dynamic fluid-structure interaction, acoustics, thermal load analysis, etc. These aspects can be treated in various ways with advanced numerical procedures. For example, in her doctoral thesis [39] , M. Marcelet, in preparation of an aerodynamic aircraft wing shape optimization, has considered a model in which the compressible Reynolds-Averaged Navier-Stokes (RANS) equations have been used to compute the three-dimensional flow about the wing, whereas the structure has been modeled as a beam subject to bending and torsion under the aerodynamic forces, and thus established the expression for the discrete gradient of aerodynamic coefficients accounting for this coupling. In this area, where functional gradients of complex coupled discrete systems are calculated, *Automatic Differentiation* as it is more and more routinely developed in tools such as Tapenade (cf. http://www-sop.inria.fr/tropics), is expected to become increasingly useful. Con-

sidering more generally the application of gradient-based methods to aerodynamic and structural wing design, the article by Leoviriyakit and Jameson [38] reflects the potentials of state-of-the-art computational methods.

In a different perspective, in the literature, the expression "multidisciplinary optimization" (MDO) most often refers to methodologies for analyzing, and locally optimizing single-discipline subsystems, and integrating them in a larger coupled system for purpose of design. In particular, the design of aeronautical complex systems has stimulated many basic developments. A commonly-used approach is the Bi-level Integrated System Synthesis (BLISS) of Sobieszczanski-Sobieski and co-authors in which the integration is organized after a distinction is made among the design variables between the global (or public) variables common to all disciplines, and the local (or private) variables associated with separate subsystems [55] [56] . A formal presentation and a comparison of collaborative optimization approaches was made by Alexandrov [4] . The DIVE approach [8] has been proposed recently as a variant of the BLISS in which the coupling between subsystems is reinforced by the solution of an additional nonlinear equation. From the original developments, MDO concepts have matured and we refer to the textbook by Keane and Nair [35] for a general presentation, and to [61] for a recent review.

In our perspective, MDO processes are viewed as game strategies [9] [44] of particular types, and our developments are linked to MDO in this light.

From the standpoint of numerical analysis, how should the public variables be optimized concurrently to account for antagonistic criteria originating from different disciplines? This article focuses on this question sometimes referred to as "*concurrent engineering*". In optimum-shape design, often the different physical phenomena are accurately modeled by partial-differential equations to be solved in domains that are identical or distinct but share a common geometrical boundary at which appropriate conditions are enforced and whose shape is to be optimized. Besides the case of the aero-structural design of an aircraft wing cited above, in the design of a stealth airplane, one would optimize the wing-shape with respect to an appropriate aerodynamic criterion, or several such criteria, concurrently with an electromagnetic criterion, such as radar cross-section

(RCS) reduction. In the latter case, both distributed PDE systems are formulated in the domain exterior to the aircraft, but have very different computational characteristics in particular concerning mesh requirements.

In the area of pure numerical simulation of multidisciplinary coupled systems, the computational cost to evaluate a configuration may be very high. *A fortiori*, in multidisciplinary optimization, one is led to evaluate a number of different configurations to iterate on the design parameters. This observation motivates the search for the most innovative and computationally efficient approaches in all the sectors of the computational chain : at the level of the solvers (using a hierarchy of physical models), the meshes and geometrical parameterizations for shape, or shape deformation, the implementation (on a sequential or parallel architecture; grid computing), and the optimizers (deterministic or semi-stochastic, or hybrid; synchronous, or asynchronous).

In the present approach, we concentrate on situations typically involving a small number of disciplines assumed to be strongly antagonistic, and a relatively moderate number of related objective functions. However, our objective functions are functionals, that is, PDE-constrained, and thus costly to evaluate. The aerodynamic and structural optimization of an aircraft configuration is a prototype of such a context, when these disciplines have been reduced to a few major objectives. This is the case when, implicitly, many subsystems are taken into account by local optimizations.

Our developments are focused on the question of approximating the Pareto set in cases of strongly-conflicting disciplines. For this purpose, a general computational technique is proposed, guided by a form of sensitivity analysis, with the additional objective to be more economical than standard evolutionary approaches.

Classically, the simplest way to account for several criteria simultaneously consists in agglomerating them all in a single performance index weighting each criterion with an appropriate coefficient, or weight. For example, with two criteria J_A and J_B, consider :

$$J = \alpha \frac{J_A}{J_A^0} + \beta \frac{J_B}{J_B^0}$$

where J_A^0 and J_B^0 are reference values, for example, those associated with an initial de-

sign. Here, α and β are positive weights to be chosen somehow. This approach is very commonly-used, particularly when one disposes of an initial design that is close to be satisfactory, that is, only a better, or slightly different optimum is to be sought. However, the construction of the agglomerated criterion involves a large amount of arbitrariness, in particular (but not only) with respect to the weights α and β that can strongly influence the result and require to be calibrated by an experienced practitioner. Thus this approach is not very general and has little physical or mathematical relevance.

An alternative to the unique criterion by agglomeration of several objective functions, consists of a two-step process in which each criterion is first optimized alone, possibly under constraints; for the above two-objective problem, one thus gets $J_A^\star$ and $J_B^\star$ as the solutions to two independent single-objective optimizations. Then, in the second step, one solves the following single-objective constrained problem :

$$\min \eta$$

where η is an auxiliary dimensionless objective-function of the same set of design variables subject to the following inequality constraints :

$$J_A \leq J_A^\star + \alpha\eta \quad \text{and} \quad J_B \leq J_B^\star + \beta\eta$$

where α and β are appropriate scales for J_A and J_B respectively. Equivalently, η is the minimum fraction for which the tolerances

$$\left(J_A - J_A^\star\right)/\alpha \leq \eta \quad \text{and} \quad \left(J_B - J_B^\star\right)/\beta \leq \eta$$

permit a trade-off solution to exist. In this alternative, assuming all the cited single-objective problems make sense separately without physical coupling, the difficulty is to treat a problem with functional inequality constraints of physically-different nature. Additionally, the same arbitrariness resides in the calibration of the weights α and β.

A real alternative to the unique agglomerated objective approach, is to establish

the front of *Pareto-optimal solutions.* To introduce this, we first recall the notion of *dominance* and *non-dominance* :

Definition : When considering the minimization of several criteria concurrently (J_A, J_B, etc), a design point $D^{(1)}$ in the parameter space is said to dominate the design $D^{(2)}$ in efficiency, which we denote as follows :

$$D^{(1)} \succ D^{(2)} ,$$

iff, for all the criteria J to be minimized, the following holds :

$$J\left[D^{(1)}\right] \leq J\left[D^{(2)}\right] ,$$

and if, for at least one criterion, the inequality is strict. Inversely, if instead :

$$D^{(1)} \not\succ D^{(2)} , \text{ and } D^{(2)} \not\succ D^{(1)} ,$$

the two design-points $D^{(1)}$ and $D^{(2)}$ are said to be non-dominated.

This notion can be used to sort a collection, or population of design-points evaluated with respect to the various criteria J_A, J_B, etc, according to the so-called *Pareto fronts*. The first front is made of all the design-points dominated by no other; the second, the front of those dominated by no other in the remaining set; etc. The result of this sorting process is sketched at Figure 1.

Relying on this sorting process, Srinivas and Deb [57] have proposed the genetic algorithm *NSGA (Non-dominated Sorting Genetic Algorithm)* which utilizes essentially the front index as the *fitness function*, the engine of the GA. Goldberg [29] improved the method by introducing a *niching* technique in order to prevent the accumulation of non-dominated design-points on a given front. To illustrate the *NSGA*, we present an experiment made by Marco *et al* [40] in which an airfoil shape was optimized to reduce drag (in transonic flow conditions) and maximize lift (in subsonic flow conditions) concurrently. The *NSGA* was implemented in two independent experiments corresponding to

finite-volume simulations of the compressible Euler equations using different meshes, one coarse and one fine. The totality of the design-points accumulated during the successive generations in the two experiments indistinctly, are represented on Figure 2 a). In each experiment, the set of design-points does not cover the entire quarter plane : not all pairs (J_A, J_B) can be achieved by the system. The boundary of the domain of realizable pairs is made of Pareto-optimal solutions. The corresponding two (discrete) fronts and the associated shapes (for the fine-mesh experiment only) are depicted on Figure 2 b) and c).

This experiment allows us to point out the principal merits and weaknesses of this approach. The method provides the designer with a rich and unbiased information on the behavior of the criteria when the parameters vary, but one can also regret the lack of hierarchy between the Pareto-optimal solutions, among which a definite operating design-point requires to be elected on the basis of some other criterion still to be introduced. Other experiments in the literature have shown that the method is very general since it has been applied to cases where the Pareto-equilibrium front was either non-convex or discontinuous. On the other hand, the computational cost of a standard application of the *NSGA* is fairly high since a large number of configurations ought to be evaluated, if an accurate identification of the front is sought. In our example, this was achieved by instantiations of a two-dimensional Eulerian flow code for purpose of demonstration; however today, realistic flow simulations about aircraft wings are based on three-dimensional turbulent Navier-Stokes equations. The cost-efficiency issue can be somewhat alleviated by the usage of parallel computing, which is possible at several levels : the parallelization of the analysis code by domain decomposition, the natural parallelization of its independent instantiations, as well as the parallelization the crossover operator in the GA [41] . Various evolutionary algorithms other than the *NSGA* have been proposed for multi-objective optimization on the basis of similar principles (e.g. *NPGA* [34] , *MOGA* [26] , *SPEA* [64] , *PAES* [37]).

When the front of Pareto-optimal solutions is convex and smooth, it may be possible to identify it point-wise, by treating all but one criterion as equality constraints, as depicted on Figure 3. However this approach is much less general since, as mentioned

before, functional constraints are difficult to handle, additionally, the identification is usually logically complex in cases involving more than two objectives.

An alternate treatment of multi-objective problems that circumvents the usually very arbitrary question of adjusting penalty constants in the agglomerated-criterion approach, and that is much more economical than an *NSGA*-type method to establish the Pareto-equilibrium front, consists in simulating a dynamic game in which the design variables are first split in complementary subsets and distributed to virtual players as individual strategies. Symmetrical as well as unsymmetrical (or hierarchical) games can be considered [44] [9] . In a symmetrical Nash game [44] , each player accommodates its own strategy to the other players strategies to optimize only one criterion. If an equilibrium point is reached, a trade-off between the various criteria is achieved.

In his doctoral thesis, B. Abou El Majd [1] has realized a number of aero-structural shape-optimization exercises related to a generic business-jet wing using either Nash or Stackelberg games, some of which are reported here for illustration, some of which have also been reported in [2] .

Here, we focus on the symmetrical formulation of Nash games involving two players A and B controlling the sub-vectors $\mathbf{y}_A$ and $\mathbf{y}_B$ composing the complete vector of design variables :

$$\mathbf{y} = (\mathbf{y}_A, \mathbf{y}_B)$$

In this case, the vector $\overline{\mathbf{y}} = (\overline{\mathbf{y}}_A, \overline{\mathbf{y}}_B)$ is said to realize a Nash equilibrium of the criteria J_A and J_B, iff :

$$\overline{\mathbf{y}}_A = \arg\min_{\mathbf{y}_A} J_A\left(\mathbf{y}_A, \overline{\mathbf{y}}_B\right)$$

and symmetrically :

$$\overline{\mathbf{y}}_B = \arg\min_{\mathbf{y}_B} J_B\left(\overline{\mathbf{y}}_A, \mathbf{y}_B\right)$$

This formulation is inspired by the negotiation mechanism of which economics and social sciences provide numerous examples.

The Nash equilibrium-point can be achieved by the following parallel algorithm [60] :

Step 1: Initialize both sub-vectors :

$$\mathbf{y}_A := \mathbf{y}_A^{(0)} \qquad \mathbf{y}_B := \mathbf{y}_B^{(0)}$$

Step 2: Perform in parallel optimization iterations of both subsystems (by independent and generally different analysis and optimization methods) :

Player A:

- Retrieve and maintain fixed

$$\mathbf{y}_B = \mathbf{y}_B^{(0)}$$

- Perform K_A minimization steps of $J_A\left(\mathbf{y}_A, \mathbf{y}_B^{(0)}\right)$ by iterating on $\mathbf{y}_A$ alone and get $\mathbf{y}_A^{(K_A)}$.

Player B:

- Retrieve and maintain fixed

$$\mathbf{y}_A = \mathbf{y}_A^{(0)}$$

- Perform K_B minimization steps of $J_B\left(\mathbf{y}_A^{(0)}, \mathbf{y}_B\right)$ by iterating on $\mathbf{y}_B$ alone and get $\mathbf{y}_B^{(K_B)}$.

Step 3: Update both sub-vectors in preparation of the information exchange :

$$\mathbf{y}_A^{(0)} := \mathbf{y}_A^{(K_A)} \qquad \mathbf{y}_B^{(0)} := \mathbf{y}_B^{(K_B)}$$

and go back to Step 2 or stop (at equilibrium).

Note that in practice, under-relaxation is very often essential to convergence. This point is particularly critical when the two criteria J_A and J_B originate from different physical disciplines associated with different dependencies and scales, as it is the case for optimum design with respect to aerodynamics and structural mechanics, or electromagnetics. However, certain rather general mathematical stabilization techniques exist; see for example [6] .

Important remark : invariance of the Nash equilibrium solution to units and scales. Assume that $\overline{\mathbf{y}} = (\overline{\mathbf{y}}_A, \overline{\mathbf{y}}_B)$ realizes a Nash equilibrium of the criteria J_A and J_B, and let Φ and Ψ be some arbitrary but smooth and strictly-monotone increasing functions; then, evidently, $\overline{\mathbf{y}}$ also realizes a Nash equilibrium of the criteria $\Phi[J_A]$ and $\Psi[J_B]$. In other words, the notion of Nash equilibrium is not only independent of the physical units used for the criteria, but also of possible changes in scales applied to them : for example, replacing J by J^α or $exp(J)$ has no effects other than a different conditioning of the numerical system. By this invariance property, the Nash game formulation contrasts outstandingly from the agglomerated criterion approach in which dimensioning the penalty constants has a strong, and usually unknown influence on the solution. The Nash equilibrium solution, unique or not, is only determined by the split of the design vector, which is here referred to as the *split of territory* by which each virtual player is allocated a subspace of action, or territory. Note that such a split is not part of the physical model, but instead an optimization strategy.

This approach has been tested successfully over a number of cases related to optimum design in aeronautics, in particular within the framework of the Jacques-Louis Lions Laboratory common to the University of Paris 6 and Dassault Aviation. One of the earliest contributions has been Wang's doctoral thesis [63] in which multi-criterion optimization problems in aerodynamics have been treated by Nash games by taking the best advantage of a distributed environment. Nevertheless, note that in some cases of multipoint drag minimization, the lift constraint was introduced by the penalty approach; thus, somewhat artificially, all the criteria were unconstrained and this results in a simplification, because it allows the Nash equilibrium to be sought from an initial point where the functional gradient is equal to zero, and the dynamic game develops in a region in which the functional is not very sensitive to parameter changes.

For purpose of illustration, we consider a two-point airfoil shape aerodynamic optimization, inspired by [60] . The targets are to maximize the lift in a subsonic regime representative of take-off and landing ($M_\infty = 0.3\,,\ \alpha = 10^o$) defining the first point, and concurrently minimize the drag in a transonic flow representative of cruise ($M_\infty = 0.8\,,\ \alpha = 2^o$)

defining the second point. For both points, the airfoil is assumed to be immersed in a compressible Eulerian flow.

For this, the airfoil boundary Γ_c is split into two complementary territories Γ_1 and Γ_2, corresponding approximately to the fore and aft regions of the airfoil. The pressure and suction sides of the airfoil are parametrized by means of two cubic B-Spline curves, each of them composed of seven basis functions, while the associated weights (control points) are the design variables of the experiment. One such design variable is allocated to either territory depending on the location of the maximum of the corresponding bell-shaped function. In this way, Γ_1 and Γ_2 are associated with specific distinct subsets of the design variables. More precisely, the two design variables located in the vicinity of the leading edge are controlled by the first player, whereas the remaining variables belong to the second one (see Figure 4, top). A trade-off between the two criteria is then sought by realizing a Nash equilibrium associated with the following formulation :

$$\min_{\Gamma_1} I_1 = \int_{\Gamma_c} p_{\text{sub}} \overrightarrow{n}\, d\Gamma \cdot \vec{e_y} \tag{1}$$

(in which the pressure field is calculated in the subsonic conditions that define the first point), and

$$\min_{\Gamma_2} I_2 = -\int_{\Gamma_c} p_{\text{trans}} \overrightarrow{n}\, d\Gamma \cdot \vec{e_x} \tag{2}$$

(in which the pressure field is calculated in the transonic conditions that define the second point).

Starting with some appropriate initial airfoil, the first player performs 5 design cycles to reduce criterion I_1 by acting only on the subset of the design variables associated with Γ_1, and maintaining the other variables fixed. The optimizer is a direct-search pattern method. In parallel, the second player performs 10 design cycles to reduce criterion I_2 by acting only on the subset of the design variables associated with Γ_2, and maintaining the other variables fixed. Then, both players exchange their best respective sub-vectors of design variables, and so on until an equilibrium is reached. The iterative convergence of this process is indicated at Figure 4 (bottom) : both criteria approach a stable asymptote.

Figure 5 illustrates a comparison of the pressure fields corresponding to the trade-off airfoil shape (Nash equilibrium solution) and the baseline airfoil. In particular, one may notice that the proposed split of territory allows the first player to enhance lifting effects by increasing the leading edge curvature (see Figure 5, top), while the second player can reduce the shock wave intensity by modifying the aft part of the airfoil shape (see Figure 5, bottom).

Another example of application of a Nash formulation to the treatment of a complex geometrical optimization problem has been given by [30] , in which two disciplines, elasticity and thermal analysis, have been considered as governing models in the competition between the structural and the cooling material topologies. This case study is given full details in the next section as an illustration of a Nash game based on a direct split of the primitive variables.

2 Concurrent structural and thermal design optimization by a split of the primitive variables

We choose a coupled heat-transfer versus thermo-elasticity system as illustrating example in concurrent design of structural mechanics. The coupled model intervenes in applications such as the nuclear safety, heat treatment, automotive and aerospace. These high technology industries express strategic needs for structures that exhibit optimal behavior under extreme thermal loads. We formulate a multidisciplinary topology design problem within the Nash game theory framework. The players are the heat equation and the thermo-elasticity system. They are given their *natural* design parameters as strategies, the heat equation controls the cooling (out of plane convection) material distribution with a minimum heat-compliance objective, and the thermo-elasticity controls the structural material distribution with a minimum structural compliance objective.

2.1 Two weakly-coupled state problems

2.1.1 Heat transfer

Let T_1 be the unknown steady state temperature distribution in the solid body, represented by the plane domain Ω, and let T_2 be the known surrounding temperature which is assumed constant in place and time. The out of plane heat flow per unit area $q_n(\mathbf{x})$ at a point $\mathbf{x} \in \Omega$ that leaves the body, is assumed to follow the constitutive law $q_n(\mathbf{x}) = \beta(T_1(\mathbf{x}) - T_2)$, where $\beta \geq 0$ is a heat transfer coefficient. If we introduce the temperature difference function $T = T_1 - T_2$, then the following elliptic boundary value problem governs the temperature distribution:

$$\begin{aligned} -\nabla \cdot (k\nabla T) + \beta\, T &= Q, \quad \text{in } \Omega, \\ T &= 0, \quad \text{on } \Gamma_T, \\ k\nabla T \cdot \mathbf{n} &= \bar{q}_n, \quad \text{on } \partial\Omega \backslash \Gamma_T. \end{aligned} \tag{3}$$

Here $\mathbf{n}$ is the outward unit normal to Ω, $k > 0$ is the heat conduction coefficient, Q is the given heat source in Ω, Γ_T is the part of $\partial\Omega$ where the temperature T_1 is prescribed to T_2, and $\bar{q}_n$ is the inward heat flux prescribed on the rest of the boundary.

Note that the coefficients k and β are not constant in Ω.

2.1.2 Thermo-elasticity

In linear isotropic thermo-elasticity the linear strains and thermal strains are given by

$$\boldsymbol{\epsilon}(\mathbf{u}) = \frac{1}{2}(\nabla \mathbf{u} + \nabla \mathbf{u}^T), \quad \boldsymbol{\epsilon}_T(T) = \alpha T\, \mathbf{I}, \tag{4}$$

in which $\mathbf{u}$ is the displacement field on Ω and α is the thermal expansion coefficient. Hooke's law states that

$$\boldsymbol{\sigma} = \mathbf{E}[\boldsymbol{\epsilon}(\mathbf{u}) - \boldsymbol{\epsilon}_T(T)], \tag{5}$$

in which $\boldsymbol{\sigma}$ is the stress tensor and $\mathbf{E}$ the elasticity tensor with standard symmetry and definiteness properties.

Given body forces $\mathbf{b}$, traction vector $\mathbf{t}$ on the boundary part $\partial\Omega\backslash\Gamma_u$, and a temperature field T, one solves for the displacement field $\mathbf{u}$ in the following elliptic boundary value problem:

$$\begin{aligned} -\nabla\cdot(\mathbf{E}[\boldsymbol{\epsilon}(\mathbf{u})-\boldsymbol{\epsilon}_T(T)]) &= \mathbf{b}, \quad \text{in } \Omega, \\ \mathbf{u} &= \mathbf{0}, \quad \text{on } \Gamma_u, \\ \mathbf{E}[\boldsymbol{\epsilon}(\mathbf{u})-\boldsymbol{\epsilon}_T(T)]\mathbf{n} &= \mathbf{t}, \quad \text{on } \partial\Omega\backslash\Gamma_u. \end{aligned} \tag{6}$$

T could be any prescribed temperature field, or the solution to the boundary value problem (3).

Note that $\mathbf{E}$, but in general not α, will later take different values at different points of Ω.

2.2 A game between heat transfer and thermo-elasticity in topology design

2.2.1 Design parameterization

In topology optimization, the design variables should take the discrete values zero or one. Due to computational reasons the design variables are relaxed to be allowed to attain values between zero and one. The intermediate values are then penalized to get close to a discrete valued design.

The material density function ρ_1, defined on Ω, should be (close to) the characteristic function for the part of Ω which is occupied by the structure characterized by heat conduction coefficient $\overline{k}$ and elasticity tensor $\overline{\mathbf{E}}$. As a consequence, we can use the following design parameterization:

$$k(\rho_1)=\rho_1^{p_1}\overline{k}, \quad \mathbf{E}(\rho_1)=\rho_1^{p_2}\overline{\mathbf{E}}, \tag{7}$$

in which p_1 and p_2 are penalization powers (to be chosen e.g. as $p_1=1$ and $p_2\approx 3$) and

$$\rho_1 = S_{R_1}(\xi_1), \tag{8}$$

where S_R is a compact linear filter operator with some "filter radius" R. The function ξ_1

is subject to the constraints

$$\epsilon_1 \leq \xi_1 \leq 1, \quad \text{a.e. in } \Omega, \quad \int_\Omega \xi_1 \, d\mathbf{x} \leq V_1, \tag{9}$$

in which ϵ_1 is a small but strictly positive and V_1 is the available volume. (One could choose $\epsilon_1 = 1$ at "no-design" places of Ω). Due to the properties of S_R, the constraints (9) hold also for the function ρ_1. The function ξ will act as the design variable in the algorithm, but the density ρ will be shown in the figures. It follows from (7) and (9) that non-presence of structure — a hole — is modeled by heat conduction coefficient $\underline{k} = \epsilon_1^{p_1}\overline{k}$ and elasticity tensor $\underline{\mathbf{E}} = \epsilon_1^{p_2}\overline{\mathbf{E}}$.

The role of the second density function ρ_2 is to indicate at what places of Ω one should apply cooling, i.e. an increased heat convection, obtained in practice e.g. by preparing the structure's surface somehow; using fins, cooling channels, fans, surface treatment for different radiation, etc. The design parameterization for β could read

$$\beta(\rho_2) = \rho_2^{p_3}\overline{\beta}, \tag{10}$$

where p_3 is yet another penalty power (one may take $p_3 = 1$), and the high level of convection is modeled by the heat transfer coefficient $\overline{\beta}$ and otherwise the convection obtained for an unprepared surface corresponds to $\beta = \underline{\beta} = \epsilon_2^{p_3}\overline{\beta}$. For $p_3 = 1$, remarkably there is no need for using a filter operator, see [30] .

The constraints for ρ_2 are the following :

$$\epsilon_2 \leq \rho_2 \leq 1, \quad \text{a.e. in } \Omega, \quad \int_\Omega \rho_2 \, d\mathbf{x} \leq V_2. \tag{11}$$

The integral constraint in (11) for ρ_2 represents a given bounded cooling resource.

We do not expect cooling at places where there is a hole. Indeed, suppose we have places where $k(\mathbf{x}) = 0$ and $Q(\mathbf{x}) = 0$. Then it follows that $T_1(\mathbf{x}) = T_2$ from the first of (3) for any small $\beta > 0$.

2.2.2 Weak formulation of the state equations

We introduce admissible spaces for the temperature field and displacement fields respectively,

$$V_T = \left\{ T \in H^1(\Omega) \mid T = 0 \text{ on } \Gamma_T \right\},$$

$$\mathbf{V}_u = \left\{ \mathbf{u} \in \mathbf{H}^1(\Omega) \mid \mathbf{u} = \mathbf{0} \text{ on } \Gamma_u \right\},$$

and the following linear and bilinear forms:

$$\begin{aligned} a_1(\rho_1, \mathbf{u}, \bar{\mathbf{u}}) &= \textstyle\int_\Omega \boldsymbol{\epsilon}(\mathbf{u}) \mathbf{E}(\rho_1) \boldsymbol{\epsilon}(\bar{\mathbf{u}}) \, d\mathbf{x}, \\ \ell_1(\rho_1, T, \bar{\mathbf{u}}) &= \textstyle\int_\Omega \boldsymbol{\epsilon}_T(T) \mathbf{E}(\rho_1) \boldsymbol{\epsilon}(\bar{\mathbf{u}}) \, d\mathbf{x} + \int_\Omega \mathbf{b} \cdot \bar{\mathbf{u}} \, d\mathbf{x} + \int_{\partial\Omega \setminus \Gamma_u} \mathbf{t} \cdot \bar{\mathbf{u}} \, ds, \end{aligned}$$

and

$$\begin{aligned} a_2(\rho_1, \rho_2, T, \bar{T}) &= \textstyle\int_\Omega k(\rho_1) \nabla T \cdot \nabla \bar{T} \, d\mathbf{x} + \int_\Omega \beta(\rho_2) T \bar{T} \, d\mathbf{x}, \\ \ell_2(\bar{T}) &= \textstyle\int_\Omega Q \bar{T} \, d\mathbf{x} + \int_{\partial\Omega \setminus \Gamma_T} \bar{q}_n \bar{T} \, ds. \end{aligned}$$

Then, the weak form for the weakly coupled state problems reads

$$\begin{aligned} &\mathbf{u} \in \mathbf{V}_u : && a_1(\rho_1, \mathbf{u}, \bar{\mathbf{u}}) &&= \ell_1(\rho_1, T, \bar{\mathbf{u}}) && \forall \bar{\mathbf{u}} \in \mathbf{V}_u, \\ &T \in V_T : && a_2(\rho_1, \rho_2, T, \bar{T}) &&= \ell_2(\bar{T}) && \forall \bar{T} \in V_T. \end{aligned} \tag{12}$$

Given ρ_1, ρ_2, the second of (12) is solved first to obtain T, and then one can solve the first of (12) to obtain also $\mathbf{u}$.

2.2.3 Formulation of the game

The player A, the thermo-elasticity system, wants to minimize compliance, i.e. the linear form from the weak formulation of the thermoelastic state problem. The strategy function of player A is the material density, in other words $\mathbf{y}_A = \rho_1$. The player B, the heat transfer system, wants to minimize "heat compliance", i.e. the linear form from the weak formulation of the heat transfer problem. The strategy function of player B is the cooling function, that is $\mathbf{y}_B = \rho_2$.

Given any pair (ρ_1, ρ_2), if we denote by $T(\rho_1, \rho_2)$ and $\mathbf{u}(\rho_1, \rho_2)$ the unique solution to

(12), then the objective functions are

$$J_A(\rho_1, \rho_2) = \ell_1(\rho_1, T(\rho_1, \rho_2), \mathbf{u}(\rho_1, \rho_2)),$$

$$J_B(\rho_1, \rho_2) = \ell_2(T(\rho_1, \rho_2)).$$

Minimizing J_A means to minimize compliance, a commonly used inverse measure of stiffness, however with loads depending on both design and temperature. Minimzing J_B means to apply cooling on the surface in such a way that a weighted integral average of the temperature is minimized.

2.2.4 FE-discretized formulation and sensitivity analyses

After FE-discretization, the system (12) reads

$$\begin{aligned} \mathbf{K}_1(\boldsymbol{\rho}_1)\mathbf{u} &= \mathbf{F}_1(\boldsymbol{\rho}_1, \mathbf{T}) \\ \mathbf{K}_2(\boldsymbol{\rho}_1, \boldsymbol{\rho}_2)\mathbf{T} &= \mathbf{F}_2 \end{aligned} \tag{13}$$

which defines implicitely functions $(\boldsymbol{\rho}_1, \boldsymbol{\rho}_2) \mapsto \mathbf{u}(\boldsymbol{\rho}_1, \boldsymbol{\rho}_2)$ and $(\boldsymbol{\rho}_1, \boldsymbol{\rho}_2) \mapsto \mathbf{T}(\boldsymbol{\rho}_1, \boldsymbol{\rho}_2)$.

The objective functions are

$$J_A(\boldsymbol{\rho}_1, \boldsymbol{\rho}_2) = \mathbf{F}_1(\boldsymbol{\rho}_1, \mathbf{T}(\boldsymbol{\rho}_1, \boldsymbol{\rho}_2))^T \mathbf{u}(\boldsymbol{\rho}_1, \boldsymbol{\rho}_2)$$

or just $J_A = \mathbf{F}_1^T \mathbf{u}$ omitting arguments, and

$$J_B(\boldsymbol{\rho}_1, \boldsymbol{\rho}_2) = \mathbf{F}_2^T \mathbf{T}(\boldsymbol{\rho}_1, \boldsymbol{\rho}_2)$$

or just $J_B = \mathbf{F}_2^T \mathbf{T}$. By implicit differentiation of the second of (13) one finds in a standard manner that

$$\frac{\partial J_B}{\partial (\boldsymbol{\rho}_2)_i} = -\mathbf{T}^T \frac{\partial \mathbf{K}_2}{\partial (\boldsymbol{\rho}_2)_i} \mathbf{T}, \tag{14}$$

omitting arguments at places, and for any i. The derivative of J_A is more involved since the right hand side of the first equation depends on the state of the second equation as

well as on the design.

We denote the partial derivative with respect to $(\boldsymbol{\rho}_1)_i$ by $'$. Omitting arguments, implicit differentiation of (13) yields

$$\begin{aligned} \mathbf{K}_1'\mathbf{u} + \mathbf{K}_1\mathbf{u}' &= \mathbf{F}_1' + (\tfrac{\partial \mathbf{F}_1}{\partial \mathbf{T}})^T\mathbf{T}', \\ \mathbf{K}_2'\mathbf{T} + \mathbf{K}_2\mathbf{T}' &= \mathbf{0}. \end{aligned} \tag{15}$$

Using the fact that $J_A = \mathbf{F}_1^T\mathbf{u} = \mathbf{u}^T\mathbf{K}_1\mathbf{u}$ one gets

$$(\mathbf{F}_1^T\mathbf{u})' = 2\mathbf{u}^T\mathbf{K}_1\mathbf{u}' + \mathbf{u}^T\mathbf{K}_1'\mathbf{u}.$$

From the first of (15) we have an expression for $\mathbf{K}_1\mathbf{u}'$, which inserted in the expression above yields

$$(\mathbf{F}_1^T\mathbf{u})' = -\mathbf{u}^T\mathbf{K}_1'\mathbf{u} + 2\mathbf{u}^T\mathbf{F}_1' + 2\mathbf{u}^T(\frac{\partial \mathbf{F}_1}{\partial \mathbf{T}})^T\mathbf{T}'. \tag{16}$$

Defining the vector $\boldsymbol{\lambda}$ according to the adjoint equation

$$\mathbf{K}_2\boldsymbol{\lambda} = \frac{\partial \mathbf{F}_1}{\partial \mathbf{T}}\mathbf{u}, \tag{17}$$

we can rewrite (16) as

$$(\mathbf{F}_1^T\mathbf{u})' = -\mathbf{u}^T\mathbf{K}_1'\mathbf{u} + 2\mathbf{u}^T\mathbf{F}_1' + 2\boldsymbol{\lambda}^T\mathbf{K}_2\mathbf{T}',$$

which, when using the expression for $\mathbf{K}_2\mathbf{T}'$ resulting from the second of (15), simplifies to

$$\frac{\partial J_A}{\partial (\boldsymbol{\rho}_1)_i} = -\mathbf{u}^T\frac{\partial \mathbf{K}_1}{\partial (\boldsymbol{\rho}_1)_i}\mathbf{u} + 2\mathbf{u}^T\frac{\partial \mathbf{F}_1}{\partial (\boldsymbol{\rho}_1)_i} - 2\boldsymbol{\lambda}^T\frac{\partial \mathbf{K}_2}{\partial (\boldsymbol{\rho}_1)_i}\mathbf{T}. \tag{18}$$

This expression, which will be used in the algorithm, contains three terms. The first one is the usual "specific energy" which results from differentiating compliance, the second term comes from design-dependent loads, and the last term comes from the fact that the load depends on the temperature which in turn is obtained by solving a heat conduction problem.

2.2.5 The computational algorithm

Starting from an initial design pair $\boldsymbol{\rho}^{(0)} = (\boldsymbol{\rho}_1^{(0)}, \boldsymbol{\rho}_2^{(0)})$:

step one$_1$: solve the problem :

$$\min_{\boldsymbol{\rho}_1} J_A(\boldsymbol{\rho}_1, \boldsymbol{\rho}_2^{(n)}) \rightarrow \boldsymbol{\rho}_1^{(n+1)}$$

step one$_2$: solve the problem :

$$\min_{\boldsymbol{\rho}_2} J_B(\boldsymbol{\rho}_1^{(n)}, \boldsymbol{\rho}_2) \rightarrow \boldsymbol{\rho}_2^{(n+1)}$$

step two : set $\boldsymbol{\rho}^{(n+1)} = (\boldsymbol{\rho}_1^{(n+1)}, \boldsymbol{\rho}_2^{(n+1)})$.

Until convergence, redo the parallel steps **one$_1$** and **one$_2$**.

The subprograms **one$_1$** and **one$_2$** are solved by means of the Moving Asymptote Method (MMA) see [59] . For each step, a complete minimization is performed using the sensitivity formulae (18) and (14) given by the previous section. A variant could be to perform only incomplete minimization, at least at the early overall iterations. In our case, this approach was tested, but did not show any better efficiency than the complete minimization of steps **one** $_1$ and **one$_2$**.

2.3 A Numerical Experiment

We consider a rectangular design domain with the dimension 1.5×1. The design domains for player J_A and J_B are presented in Figure 6.

The thermo-elasticity setting is as follows. The right and left side of the domain are fixed. A vertical load is applied in the middle of the lower boundary. For heat transfer, a heat source Q is supplying heat within a restricted area around the point where the force of the thermoelastic problem is acting. The temperature is prescribed along the right and left boundary. The upper and lower boundaries are considered isolated. Only the

left half of the structure is considered for the computations due to symmetry. Identical meshes consisting of 45×60 uniform 9-noded biquadratic elements are used for the two players.

The optimal topologies after 6 (overall loop) iterations are shown in Figure 7.

Black area indicates material i.e. $\rho_i = 1$.

The topology of player J_A can be characterized as a structure consisting of two legs. One thick leg attached to the upper side of the design domain and running down to the center of the lower boundary where it meets the other part of the leg. The second leg is attached to the lower corners of the design domain and runs like an arc from one side to the other. For the purely elastic problem with no temperature strains the topology will consist only of one thick leg. This leg runs from the upper corners down to the point in the center of the lower boundary where the load is acting. Increasing the temperature will result in the creation of the second leg. This second leg gets thicker for higher temperatures at the expense of the upper leg which gets thinner and the point where the leg is attached to the boundary is lowered. Comparable topologies and behavior are presented by [51] .

The topology of player J_B after the first iteration has a half circle shape and is concentrated around the heat source. After that ρ_1 has been updated there is a drastic change in the topology. The distribution of ρ_2 follows the temperature distribution which in turn follows the topology of player J_A. In Figure 7 the Nash equilibrium topology of player J_B is aligned to the one of player J_A.

In order to compare the Nash game solution to those obtained by minimization of a weighted objective, we introduce the scalar objective

$$j_\lambda(\rho_1, \rho_2) = \lambda J_A(\rho_1, \rho_2) + (1 - \lambda) J_B(\rho_1, \rho_2).$$

We have optimized j_λ for different values of $\lambda \in [0, 1]$.

The optimal solution for $\lambda = 0.5$ is presented in Figure 8.

From the results presented in table-1, it is observed that the optima of j_λ are slightly

	$\lambda = 0.333$	$\lambda = 0.5$	$\lambda = 0.667$	NE
J_A	15.6	15.0	14.3	13.3
J_B	0.631	0.639	0.651	0.743

Table 1: Comparison between the Nash equilibrium and weighted optima.

dependent on the weights. By a simple extrapolation, it appears as if the Nash game has selected a particular value of λ quite close to 1 (if we assume that the NE is *on the convex Pareto Front* which is of course not guaranteed). The Nash game solution for this example favored the player which controls the structure. This fact was never explicitly stated. One explanation to this result could be that we do not have an even coupling between the heat transfer and the thermo-elasticity state equations. The strategy controlled by the structure, ρ_1, intervenes in both of the state equations. The strategy controlled by the heat, ρ_2, does only explicitly intervene in the state equation for the heat transfer.

We have *split* the two parameters ρ_1 and ρ_2 in what we termed *natural* splitting. It may happen that in some industrial areas, the structural and the heat transfer function specifications are really the -concurrent- tasks of -concurrent- divisions (which may even not be part of the same firm). In this case, the above splitting, be it natural or not, is simply an imposed rule of the game played by the two divisions. In less constrained frameworks, the asymmetric role played by parameters and the strong dependence of the Nash equilibria on the splitting choice, makes the natural splitting quite questionable.

In the next section, we address an important facet of the difficult problem of efficient choice of territory splitting.

3 Nash game by adaptive split of territory

As we have seen in Section 2, and referring also to [60] , in PDE-constrained optimization, the Nash game formulation has the following most important merits :

1. the iteration applies to a set of design variables, and not to a population of such vectors;

2. it permits straightforwardly to couple physical disciplines represented by indepen-

dent codes through the exchange of design variables;

3. parallel computing can be exploited readily;

4. the multi-objective solution satisfies the above property of invariance to units and scales.

Keeping the above example in mind, we return now to our general discussion on multi-objective, or multidiscipline optimization. In optimum-shape design in aerodynamics, we are facing two major difficulties.

The first difficulty is related to the fact that only the simulation of a complex flow by a high-fidelity model (e.g. by the RANS equations) can provide a reliable evaluation of the aerodynamic coefficients. For instance, the solution of the three-dimensional compressible Euler equations, not so long ago considered as an accomplishment, only provides the wave drag and friction forces are neglected, as well as turbulence effects. The computational cost of an accurate evaluation of the aerodynamic functionals is thus very high.

Secondly, by nature, transonic flows are only weak solutions to the partial-differential equations of gasdynamics. As such, they are very sensitive to variations in boundary conditions, such as shape variations. The aerodynamic performance is therefore very fragile, in particular drag, and tolerance margins are small. By coupling aerodynamics with one or more other disciplines in a multidisciplinary optimization, it is imperative to maintain the aerodynamic performance near the optimal level.

This observation has led us to introduce the notion of *primary functional* with respect to which sub-optimality should be maintained, and *secondary functional* to be reduced under possible constraints.

In our notations, the dimension of the full design space is N. A first optimization step is completed in which the sole principal criterion J_A is minimized with respect to the totality of the N design variables, yielding a vector $\mathbf{y}_A^\star$ that realizes, by hypothesis, a local or global minimum of this criterion. It is also assumed that at this point, K ($K < N$) scalar constraints ($g_k = 0$, $k = 1, 2, ..., K$, or more compactly $\mathbf{g} = 0$) are active. Then, one wishes to conduct a second optimization step, multi-objective and competitive

in nature, by establishing a Nash equilibrium between the criteria J_A and J_B. To extend the formulation of the previous experiment, the following more general *split of territory* is introduced :

$$\mathbf{y} = \mathbf{y}\left(\mathbf{u}, \mathbf{v}\right) = \mathbf{y}_A^\star + \mathbf{S} \begin{bmatrix} \mathbf{u} \\ \\ \mathbf{v} \end{bmatrix} \tag{19}$$

where :

$$\mathbf{u} = \begin{bmatrix} u_1 \\ \vdots \\ u_{N-p} \end{bmatrix}, \quad \mathbf{v} = \begin{bmatrix} v_p \\ \vdots \\ v_1 \end{bmatrix} \tag{20}$$

in which $\mathbf{S}$ is an adjustable matrix of dimension $N \times N$, referred to as the *splitting matrix*, and to utilize the sub-vectors $\mathbf{u}$ ($\mathbf{u} \in \mathbb{R}^{N-p}$) and $\mathbf{v}$ ($\mathbf{v} \in \mathbb{R}^p$) as strategies, or territories of two virtual players A and B in charge of the minimization of J_A and J_B respectively.

The Nash equilibrium point, if it exists, is denoted $\overline{\mathbf{y}} = \mathbf{y}\left(\overline{\mathbf{u}}, \overline{\mathbf{v}}\right)$, and it is associated with the following coupled optimization problems :

$$\begin{cases} \min\limits_{\mathbf{u} \in \mathbb{R}^{N-p}} J_A\Big[\, \mathbf{y}\left(\mathbf{u}, \overline{\mathbf{v}}\right) \Big] \\ \text{Subject to :} \;\; \mathbf{g}\Big[\, \mathbf{y}\left(\mathbf{u}, \overline{\mathbf{v}}\right) \Big] = 0 \end{cases} \tag{21}$$

and :

$$\begin{cases} \min\limits_{\mathbf{v} \in \mathbb{R}^p} J_B\Big[\, Y\left(\overline{\mathbf{u}}, \mathbf{v}\right) \Big] \\ \text{Subject to : no constraints} \end{cases} \tag{22}$$

The dimension p of sub-vector $\mathbf{v}$ which controls the subspace of action of player B is adjustable ($p \geq 1$); however, the dimension $N - p$ of sub-vector $\mathbf{u}$ must be at least equal to 1, and at least equal to the number K ($K \geq 0$) of active constraints; this gives the following bounds on p :

$$1 \leq p \leq N - \max(K, 1) \tag{23}$$

In the limiting case ($N - p = K$), in the above Nash game formulation, the minimization of J_A under constraints reduces to the adjustment of the K components of sub-vector $\mathbf{u}$ to satisfy the K scalar constraints. This case has been examined in [16]. Hereafter,

unless mentioned otherwise, a strict inequality is assumed instead.

In the examples cited above [63] [60] , the split is a partition of the *primitive variables*, that is, the original components of the design vector Y. Our new formulation encompasses this particular case obtained when the splitting matrix is a permutation matrix, and much more general alternatives as well.

In a parametric shape optimization, the primitive variables are geometrical control parameters, such as the weights put on the different Hicks-Henne basis functions, or the coordinates of control points in a Bézier or B-spline parameterization. Thus, typically, these variables are associated with specific locations of the optimized geometry. Hence, when the splitting is a permutation, the permutation reflects our intuitive understanding of the dependency of the physical functionals on the geometry, or regions of it. For instance, in the example of Figure 4, the split was guided by the knowledge that in a transonic flow, the wave drag is the result of the shock intensity and it depends mostly on the delicate design of the geometry on the upper surface near the shock, whereas, in a subsonic flow, the lift is essentially proportional to the airfoil thickness. In his doctoral thesis, Wang [63] demonstrated that iterations based on choices for the splitting opposite to this physical sense, unsurprisingly, diverge.

These considerations lead us to raise the following question : how should the split be defined in a general and systematic manner to respect the physical sense? In particular, if the Nash game is initiated from a viable, physically-relevant solution corresponding to an optimum of the primary criterion J_A, can near-optimality of this criterion be maintained at equilibrium?

With the formulation of (19), the subspace spanned by the first $N-p$ column vectors of the splitting matrix $\mathbf{S}$ can be viewed as the territory assigned to player A in charge of minimizing the primary criterion J_A, and the subspace spanned by the last p column vectors as the territory assigned to player B in charge of minimizing the secondary criterion J_B. Thus the above open questions are those of the adequacy of the split of territory. The option which is adopted here consists in making this choice statically (and not adaptively in the course of the dynamic game), at completion of the first step of the

procedure in which the primary criterion is minimized alone (possibly under constraints) in full dimension N, yielding the optimal design vector $\mathbf{y}_A^\star$, and before any competitive strategy is initiated. Thus the choice is made, here once for all, on the basis of the analysis of the sensitivity of this criterion only. We specifically enforce the following condition : the second step of the optimization procedure, the competitive step, should be such that infinitesimal perturbations of the parameters about $\mathbf{y}_A^\star$ that lie in the subspace identified as the territory of the secondary criterion should cause the least possible degradation of the primary criterion (with respect to the minimum achieved at completion of the first step). As a basis for the identification of the optimal splitting, one considers the formal Taylor's expansion of the primary functional to second order about $\mathbf{y}_A^\star$ in the direction of a unit vector $\Omega \in \mathbb{R}^N$:

$$J_A\left(\mathbf{y}_A^\star + \epsilon\boldsymbol{\omega}\right) = J_A\left(\mathbf{y}_A^\star\right) + \epsilon\,\nabla J_A^\star\,.\,\boldsymbol{\omega} + \frac{\epsilon^2}{2}\,\boldsymbol{\omega}\,.\,\mathbf{H}_A^\star\,\boldsymbol{\omega} + O(\epsilon^3) \tag{24}$$

where $\mathbf{H}_A^\star$ denotes the Hessian matrix of J_A at $\mathbf{y} = \mathbf{y}_A^\star$. Our goal is to propose a sensible splitting associated with the definition of a vector basis $\{\,\boldsymbol{\omega}^k\,\}$ $(k = 1, ..., N)$. To fix the ideas, let us assume that the first few elements, $\{\,\boldsymbol{\omega}^k\,\}$ $(k = 1, 2, ...)$, of the basis are dedicated to player A in charge of reducing the primary criterion J_A, and inversely, the tail elements, $\{\,\boldsymbol{\omega}^k\,\}$ $(k = N, N-1...)$, to player B in charge of reducing the secondary criterion J_B. Note that the direction of maximum sensitivity of the primary criterion J_A, or steepest-descent direction, is given by the gradient, $\nabla J_A^\star$ at $\mathbf{y} = \mathbf{y}_A^\star$. Thus, the following two conditions should be satisfied by the basis :

1. the first few elements should span the gradient, $\nabla J_A^\star$;

2. inversely, the difference $|J_A\left(\mathbf{y}_A^\star + \epsilon\boldsymbol{\omega}\right) - J_A\left(\mathbf{y}_A^\star\right)|$, when ϵ is small and fixed, should be as small as possible when $\boldsymbol{\omega}$ is a tail element of the basis.

At $\mathbf{y} = \mathbf{y}_A^\star$, the optimality conditions imply that the gradient $\nabla J_A^\star$ is a linear combination of the K active constraint gradients, the coefficients being the Lagrange multipliers. Thus a way to achieve the first condition is to enforce that the first K elements of the basis have the same span as the gradients of the K active constraints. For this, one

requires that $\{\,\boldsymbol{\omega}^k\,\}$ $(k=1,2,...,K)$ be the result of applying the Gram-Schmidt orthogonalization process to the constraint gradients $\{\,\nabla g_k^\star\,\}$ $(k=1,2,...,K)$. Then, let $\mathbf{P}$ be the following projection matrix :

$$\mathbf{P} = \mathbf{I} - \sum_{k=1}^{K} \left[\boldsymbol{\omega}^k\right] \left[\boldsymbol{\omega}^k\right]^T \tag{25}$$

where $\left[\boldsymbol{\omega}^k\right]$ denotes the column-vector matrix made of the components of vector $\boldsymbol{\omega}^k$, and consider the following real-symmetric matrix :

$$\mathbf{H}'_A = \mathbf{P}\,\mathbf{H}^\star_A\,\mathbf{P} \tag{26}$$

We claim that the eigenvectors of the matrix $\mathbf{H}'_A$, ordered appropriately, constitute the best choice.

First, these eigenvectors contain the null space of the projection matrix $\mathbf{P}$, that is, $\{\,\boldsymbol{\omega}^k\,\}$ $(k=1,2,...,K)$. Thus the first condition is satisfied simply if the ordering is such that these vectors appear first.

Second, the basis is orthogonal; hence the tail elements are orthogonal to the first K, and to $\nabla J_A^\star$ as a consequence of the first condition. Thus, for $\boldsymbol{\omega} = \boldsymbol{\omega}^k$ $(k \geq K+1)$, the principal term in the expansion of the difference, $|J_A\,(\mathbf{y}_A^\star + \epsilon\boldsymbol{\omega}) - J_A\,(\mathbf{y}_A^\star)|$ is the quadratic term. This term, including the absolute value, reduces to the Rayleigh quotient associated with the matrix $\mathbf{H}'_A$ (assuming positive-definiteness), and the classical characterization of eigenvectors, here by decreasing eigenvalue, holds. □

Starting from the above observations, the following theorem, taken from [16] , exploits this basic principle and draws certain additional consequences related to the Nash game. It is assumed that the two criteria J_A and J_B are strictly positive and such that :

$$J_A^\star = J_A\,(\mathbf{y}_A^\star) > 0\,, \quad J_B^\star = J_B\,(\mathbf{y}_A^\star) > 0 \tag{27}$$

If necessary the problem can easily be reformulated to meet these requirements.

Theorem 1. *Let N, p and K be positive integers such that :*

$$1 \leq p \leq N - \max(K, 1) \tag{28}$$

Let J_A, J_B and, if $K \geq 1$, $\{ g_k \}$ $(1 \leq k \leq K)$, be $K + 2$ smooth real-valued functions of the vector $Y \in \mathbb{R}^N$. Assume that J_A and J_B are positive, and consider the following primary optimization problem,

$$\min_{Y \in \mathbb{R}^N} J_A(\mathbf{y}) \tag{29}$$

that is either unconstrained ($K = 0$), or subject to the following K equality constraints :

$$\mathbf{g}(\mathbf{y}) = (g_1, g_2, ..., g_K)^T = 0 \tag{30}$$

Assume that the above minimization problem admits a local or global solution at a point $\mathbf{y}_A^\star \in \mathbb{R}^N$ at which $J_A^\star = J_A(\mathbf{y}_A^\star) > 0$ and $J_B^\star = J_B(\mathbf{y}_A^\star) > 0$, and let $\mathbf{H}_A^\star$ denote the Hessian matrix of the criterion J_A at $\mathbf{y} = \mathbf{y}_A^\star$.

If $K = 0$, let $\mathbf{P} = \mathbf{I}$ and $\mathbf{H}'_A = \mathbf{H}_A^\star$; otherwise, assume that the constraint gradients, $\{ \nabla g_k^\star \}$ $(1 \leq k \leq K)$, are linearly independent and apply the Gram-Schmidt orthogonalization process to the constraint gradients, and let $\{ \boldsymbol{\omega}^k \}$ $(1 \leq k \leq K)$ be the resulting orthonormal vectors. Let $\mathbf{P}$ be the matrix associated with the projection operator onto the K-dimensional subspace tangent to the hyper-surfaces $g_k = 0$ $(1 \leq k \leq K)$ at $\mathbf{y} = \mathbf{y}_A^\star$,

$$\mathbf{P} = \mathbf{I} - \sum_{k=1}^{K} \left[\boldsymbol{\omega}^k \right] \left[\boldsymbol{\omega}^k \right]^T \tag{31}$$

where $\left[\boldsymbol{\omega}^k \right]$ denotes the column-vector matrix made of the components of vector $\boldsymbol{\omega}^k$, and consider the following real-symmetric matrix :

$$\mathbf{H}'_A = \mathbf{P}\, \mathbf{H}_A^\star\, \mathbf{P} \tag{32}$$

Let $\boldsymbol{\Omega}$ be an orthogonal matrix whose column-vectors are normalized eigenvectors of the matrix $\mathbf{H}'_A$ organized in such a way that the first K are precisely $\{ \boldsymbol{\omega}^k \}$ $(1 \leq k \leq K)$,

and the subsequent $N-K$ are arranged by decreasing order of the eigenvalue

$$h'_k = \boldsymbol{\omega}^k \,.\, \mathbf{H}'_A \, \boldsymbol{\omega}^k = \boldsymbol{\omega}^k \,.\, \mathbf{H}^\star_A \, \boldsymbol{\omega}^k \quad (K+1 \leq k \leq N) \tag{33}$$

Consider the splitting of parameters defined by :

$$\mathbf{y} = \mathbf{y}^\star_A + \boldsymbol{\Omega} \begin{bmatrix} \mathbf{u} \\ \\ \mathbf{v} \end{bmatrix}, \quad \mathbf{u} = \begin{bmatrix} u_1 \\ \vdots \\ u_{N-p} \end{bmatrix}, \quad \mathbf{v} = \begin{bmatrix} v_p \\ \vdots \\ v_1 \end{bmatrix} \tag{34}$$

Let ε be a small positive parameter ($0 \leq \varepsilon \leq 1$), and let $\overline{\mathbf{y}}_\varepsilon$ denote the Nash equilibrium point associated with the concurrent optimization problem :

$$\begin{cases} \min\limits_{\mathbf{u} \in \mathbb{R}^{N-p}} J_A \\ \\ \textit{Subject to :} \ \mathbf{g} = 0 \end{cases} \quad \textit{and} \quad \begin{cases} \min\limits_{\mathbf{v} \in \mathbb{R}^{p}} J_{AB} \\ \\ \textit{Subject to : no constraints} \end{cases} \tag{35}$$

in which again the constraint $\mathbf{g} = 0$ is not considered when $K = 0$, and

$$J_{AB} := \frac{J_A}{J^\star_A} + \varepsilon \left(\theta \, \frac{J_B}{J^\star_B} - \frac{J_A}{J^\star_A} \right) \tag{36}$$

where θ is a strictly-positive relaxation parameter ($\theta \leq 1$ for under-relaxation).

Then :

- *[Optimality of orthogonal decomposition] If the matrix $\mathbf{H}'_A$ is positive semi-definite, which is the case in particular if the primary problem is unconstrained ($K = 0$), or if it is subject to linear equality constraints, its eigenvalues have the following structure :*

$$h'_1 = h'_2 = ... = h'_K = 0 \quad h'_{K+1} \geq h'_{K+2} \geq ... \geq h'_N \geq 0 \tag{37}$$

and the tail associated eigenvectors $\{ \boldsymbol{\omega}^k \}$ ($K+1 \leq k \leq N$) have the following

variational characterization :

$$\begin{aligned}
\boldsymbol{\omega}^N &= \arg\min_{\boldsymbol{\omega}} \; |\boldsymbol{\omega} \,.\, \mathbf{H}_A^\star \, \boldsymbol{\omega}| \;\; s.t. \;\; \|\boldsymbol{\omega}\| = 1 \;\; and \;\; \boldsymbol{\omega} \perp \left\{\boldsymbol{\omega}^1, \boldsymbol{\omega}^2, ..., \boldsymbol{\omega}^K\right\} \\
\boldsymbol{\omega}^{N-1} &= \arg\min_{\boldsymbol{\omega}} \; |\boldsymbol{\omega} \,.\, \mathbf{H}_A^\star \, \boldsymbol{\omega}| \;\; s.t. \;\; \|\boldsymbol{\omega}\| = 1 \;\; and \;\; \boldsymbol{\omega} \perp \left\{\boldsymbol{\omega}^1, \boldsymbol{\omega}^2, ..., \boldsymbol{\omega}^K, \boldsymbol{\omega}^N\right\} \\
\boldsymbol{\omega}^{N-2} &= \arg\min_{\boldsymbol{\omega}} \; |\boldsymbol{\omega} \,.\, \mathbf{H}_A^\star \, \boldsymbol{\omega}| \;\; s.t. \;\; \|\boldsymbol{\omega}\| = 1 \;\; and \;\; \boldsymbol{\omega} \perp \left\{\boldsymbol{\omega}^1, \boldsymbol{\omega}^2, ..., \boldsymbol{\omega}^K, \boldsymbol{\omega}^N, \boldsymbol{\omega}^{N-1}\right\} \\
&\vdots
\end{aligned} \tag{38}$$

- *[Preservation of optimum point as a Nash equilibrium] For $\varepsilon = 0$, a Nash equilibrium point exists and it is :*

$$\overline{\mathbf{y}}_0 = \mathbf{y}_A^\star \tag{39}$$

- *[Robustness of original design] If the Nash equilibrium point $\overline{\mathbf{y}}_\varepsilon$ exists for $\varepsilon > 0$ and sufficiently small, and if it depends smoothly on this parameter, the functions :*

$$j_A(\varepsilon) = J_A\left(\overline{\mathbf{y}}_\varepsilon\right) \,, \quad j_{AB}(\varepsilon) = J_{AB}\left(\overline{\mathbf{y}}_\varepsilon\right) \tag{40}$$

are such that :

$$j'_A(0) = 0 \,, \quad j'_{AB}(0) = \theta - 1 \leq 0 \tag{41}$$

and

$$j_A(\varepsilon) = J_A^\star + O(\varepsilon^2) \,, \quad j_{AB}(\varepsilon) = 1 + (\theta - 1)\,\varepsilon + O(\varepsilon^2) \tag{42}$$

- *In case of linear equality constraints, the Nash equilibrium point satisfies identically :*

$$u_k(\varepsilon) = 0 \quad (1 \leq k \leq K) \tag{43}$$

$$\overline{\mathbf{y}}_\varepsilon = \mathbf{y}_A^\star + \sum_{k=K+1}^{N-p} u_k(\varepsilon)\, \boldsymbol{\omega}^k + \sum_{j=1}^{p} v_j(\varepsilon)\, \boldsymbol{\omega}^{N+1-j} \tag{44}$$

- *For $K = 1$ and $p = N - 1$, the Nash equilibrium point $\overline{\mathbf{y}}_\varepsilon$* is Pareto optimal.

We have seen already why the proposed basis of eigenvectors is optimal for the problem raised by the case of a preponderant or fragile discipline, in relation with the performance

of the Nash equilibrium solution; shortly speaking, the spliiting is such that a minimal degradation of J_A is caused by the reduction of J_B. Another aspect is the existence itself of this equilibrium. With respect to this, and without entering all the details of the full proof, given in [16], let us examine the mechanism by which the present choice of territory splitting also permits to guarantee the preservation of initial optimum point of discipline A alone, $\mathbf{y}_A^\star$, as a Nash equilibrium of the above formulation for $\varepsilon = 0$, as stated in (39).

For $\varepsilon = 0$, let the criterion $J_A = J$ for notational simplicity. The criteria J_{AB} and J are functionally proportional, and so are their gradients. We wish to establish that $\overline{\mathbf{u}} = \overline{\mathbf{v}} = 0$, or equivalently $\mathbf{y} = \mathbf{y}_A^\star$, indeed corresponds to a Nash equilibrium.

On one side, for fixed $\mathbf{v} = \overline{\mathbf{v}} = 0$, the sub-vector $\mathbf{u} = 0$ indeed realizes the minimum of $J_A = J$ subject to the constraint $\mathbf{g} = 0$, because this optimization of $\mathbf{u}$ is equivalent to the minimization of J_A in a subset that contains the (global) solution $\mathbf{y}_A^\star$ of the minimization in the full design space.

On the other side, for fixed $\mathbf{u} = \overline{\mathbf{u}} = 0$, the (unconstrained) derivative of J_{AB} with respect to an arbitrary component v_k $(1 \leq k \leq p)$ of the sub-vector $\mathbf{v}$ is proportional to :

$$\frac{\partial J}{\partial v_k} = \nabla J \,.\, \frac{\partial \mathbf{y}}{\partial v_k} = \nabla J_A^\star \,.\, \boldsymbol{\omega}^{N-k+1} = 0$$

The above result is justified as follows: firstly, the optimality condition requires that the gradient $\nabla J_A^\star$ be a linear combination of the constraint gradients, the coefficients of which are the Lagrange multipliers; secondly, these constraint gradients are in the span of the first K column-vectors of the splitting matrix $\boldsymbol{\Omega}$ (by construction of this matrix), and thus so is $\nabla J_A^\star$; thirdly, the scalar product is made with a tail column-vector $(N-k+1 > N-p)$ of the same orthogonal matrix. In this resides the key element of our construction of the splitting matrix, $\boldsymbol{\Omega}$. Hence, for fixed $\mathbf{u} = \overline{\mathbf{u}} = 0$, the unconstrained criterion $J_{AB} \sim J$ is also stationary with respect to sub-vector $\mathbf{v}$ at $\mathbf{v} = \overline{\mathbf{v}} = 0$.

In addition to the stationarity of the two sub-problems, the local convexity of the sub-problems can be established by arguments omitted here. Thus, the first conclusion is that the Nash-equilibrium point $\overline{\mathbf{y}}_0$ exists and it is equal to $\overline{\mathbf{y}}_A^\star$. $\square$

As a consequence, under appropriate regularity conditions, we assume that a continuum of Nash-equilibrium points exists, parameterized by ε, $\{\overline{\mathbf{y}}_\varepsilon\}$, originating from the single-discipline A optimum design-point, $\overline{\mathbf{y}}_0 = \mathbf{y}_A^\star$. Let us now examine how the criteria in (40) evolve along this continuum. For this, first observe that the nonlinear constraint is satisfied along the continuum:

$$\forall \varepsilon \ : \ \mathbf{g}(\overline{\mathbf{y}}_\varepsilon) = 0 \tag{45}$$

Differentiating this equation and setting ε to 0 give:

$$\forall k = 1, 2, \ldots, K \ : \ \nabla g_k^\star \,.\, \overline{\mathbf{y}}_0' = 0 \tag{46}$$

where $'$ indicates differentiation with respect to ε. Besides, the optimality condition at $\varepsilon = 0$ writes

$$\nabla J_A^\star + \sum_{k=1}^{K} \lambda_k \nabla g_k^\star = 0 \tag{47}$$

where $\{\lambda_k\}$ are Lagrange multipliers. Consequently:

$$j_A'(0) = \nabla J_A^\star \,.\, \overline{\mathbf{y}}_0' = 0 \tag{48}$$

which establishes the first equation in (41); the second is then derived straightforwardly by letting $j_\theta(\varepsilon) = \theta J_B(\overline{\mathbf{y}}_\varepsilon)/J_B^\star - j_A(\varepsilon)/J_A^\star$, differentiating $j_{AB}(\varepsilon) = j_A(\varepsilon)/J_A^\star + \varepsilon j_\theta(\varepsilon)$ with respect to ε and setting $\varepsilon = 0$; this gives:

$$j_{AB}'(0) = j_\theta(0) = \theta - 1 \tag{49}$$

Then, (42) is a direct consequence. $\square$

In summary, this theorem establishes two main achievements related to the Nash equilibrium solution :

- A potential performance result : it permits to identify abstractly an orthogonal decomposition of the parameter-space that is such that for given dimension p ($p \leq$

$N - \max(K, 1)$), the tail p vectors of the basis correspond to the directions of least variation of the primary functional J_A from its minimum value under possible equality constraints; in this sense, these eigenvectors span the subspace of dimension p in which the primary functional is the most insensitive to the small variations in the design vector that will be made, in a second phase of optimization, to reduce a secondary functional, J_B;

- An existence result : a procedure involving a continuation parameter ε ($0 \leq \varepsilon \leq 1$) has been set up permitting to introduce gradually and smoothly the secondary functional J_B in competition with the primary functional J_A in a Nash game; for $\varepsilon = 0$, it is established that the original optimal solution $\mathbf{y}_A^\star$ is a Nash equilibrium point of the initially-trivial game formulation; consequently, by continuity, the Nash equilibrium solution exists, at least for ε sufficiently small. Another parameter θ appears in the formulation; it allows under or over-relaxation of the process; if $\theta < 1$, the auxiliary criterion J_{AB} at the Nash equilibrium point $\overline{\mathbf{y}}_\varepsilon$ decreases when ε increases, but remains sufficiently small; since $\overline{\mathbf{y}}_0 = \mathbf{y}_A^\star$, the locus of $\overline{\mathbf{y}}_\varepsilon$ as ε varies is viewed as a continuation of the original optimum point of the primary functional alone.

The construction of the orthogonal basis is made at full convergence of the minimization of the primary functional by diagonalization of the Hessian matrix restricted to the subspace tangent to the hypersurfaces representing the active constraints. To identify this tangent subspace, a Gram-Schmidt orthogonalization process is applied to the constraint gradients. In practice, the Hessian can be calculated exactly either formally or by automatic differentiation; otherwise, an approximation can be made by differentiating a *meta-model* for the primary functional and constraints valid in a neighborhood of the optimal solution $\mathbf{y}_A^\star$. This meta-model can be, for example, an artificial neural network or a Kriging model (see for instance [14] [22]) .

We close this section by emphasizing again the merit of our formulation, when equality constraints are active, to remain consistent with the single-criterion minimization of the primary functional alone at the initial point $\varepsilon = 0$ of the continuation procedure ($\overline{\mathbf{y}}_0 =$

$\mathbf{y}_A^\star$). This nontrivial property usually does not hold when the split is made over the primitive variables as formerly proposed in [63] [60] , unless the constraints are treated by the penalty approach. The variations in the primary functional are initially second-order in ε; thus the new formulation permits to identify smoothly the locus of Nash equilibrium solutions as ε varies, by an algorithm whose iterative convergence is facilitated by this robustness property, since the potential antagonism between the two criteria can be introduced as smoothly as necessary by small enough steps in the continuation parameter ε.

4 Application of territory splitting to the aero-structural shape optimization of a business jet wing

In order to illustrate the influence of the split of territory on the result of a practical two-discipline optimization, the main results achieved by B. Abou El Majd in his doctoral thesis [1] concerning a case of aero-structural shape optimization of a business jet wing, also in [2], are reproduced here. In his thesis, a number of algorithmic variants, including some whose formulations rely on a hierarchical Stackelberg game (instead of a symmetrical Nash game), have been described in details, tested and analyzed systematically.

Aerodynamics is treated as the preponderant discipline; it will also reveal to be a fragile discipline. The flow about the wing is computed by a finite-volume simulation of the three-dimensional Euler equations. The method handles unstructured grids by the construction of a dual finite-volume mesh, whose generic cell is around a node and its boundary is made of portions of medians of the elements. The approximation scheme relies on a Roe-type upwind solver. The computation yields the wave drag coefficient, C_D, as well as other aerodynamic coefficients, such as lift, C_L. The simulation point is transonic ($M_\infty = 0.83$, $\alpha = 2^o$). The primary objective is to minimize the drag coefficient augmented by a penalty term which is active when a minimal lift coefficient constraint is

violated. Thus, the primary criterion admits the following expression :

$$J_A = \frac{C_D}{C_{D_0}} + 10^4 \max\left(0, 1 - \frac{C_L}{C_{L_0}}\right) \tag{50}$$

in which the reference quantities, indicated by the subscript $_0$ correspond to an initial geometry defined by an initial three-dimensional unstructured grid about the wing.

Throughout the optimization process, the geometry is iteratively modified according to the so-called *Free-Form Deformation (FFD)* method which originates from computer vision, and was proposed in the context of an aero-structural design loop by Samareh [53]. In this approach, a formula is given *a priori*, in a closed form involving adjustable parameters, to a three-dimensional *deformation field*, formally and independently of the discrete or continuous representation of the geometry itself, here an unstructured volume mesh. By construction, the deformation field is made to be smooth and equal to zero outside of a support, which is usually a bounding box of simple shape whose boundaries are not made in general of meshpoints. At a given optimization iteration, the deformation field is redefined and applied to the meshpoints lying inside the support, thus permitting an update of the surface meshpoints, but also of meshpoints in the computed volume in the vicinity of the optimized surface. In this way, an initial unstructured volume mesh evolves according to a deformation defined explicitly in terms of the *FFD* parameters. These parameters are taken to be the design variables of the optimization loop and they are updated here according to the Nelder-Mead [45] simplex method to reduce the above criterion J_A.

This procedure results in a simple and fairly robust iterative algorithm. In our experience, this procedure is less subject to mesh overlapping than a volume mesh reconstruction from the displacement of the boundary meshpoints by a pseudo-elasticity equation, such as the spring method.

In our experiments, a system of generalized coordinates (ξ, η, ζ) is defined and corresponds to longitudinal, vertical and span-wise directions.When the bounding box is a parallelepiped, the transfinite interpolation of the Cartesian coordinates suffices to define these transformed coordinates throughout the box. Then, the deformation field is defined

as a linear combination of products of three Bernstein polynomials of these coordinates. Precisely, an arbitrary point $\mathbf{q}$ is given the following displacement $\Delta\mathbf{q}$:

$$\Delta\mathbf{q} = \sum_{i=0}^{n_i} \sum_{j=0}^{n_j} \sum_{k=0}^{n_k} B_{n_i}^i(\xi_q)\, B_{n_j}^j(\eta_q)\, B_{n_k}^k(\zeta_q)\, \Delta P_{ijk} \tag{51}$$

in which, for the kth Bernstein polynomial of degree n,

$$B_n^k(t) = \frac{n!}{k!\,(n-k)!}\, t^k\, (1-t)^{n-k} \tag{52}$$

The degrees of the parameterization in the three physical directions, (n_i, n_j, n_k), are fixed, and the vector-valued weighting coefficients $\{\Delta P_{ijk}\}$ $(0 \leq i \leq n_i\ ,\ 0 \leq j \leq n_j,\ 0 \leq k \leq n_k)$ are the design variables of the optimization. Such a geometrical parameterization generalizes the Bézier curve formula, and combined with the classical degree-elevation process, it facilitates the construction of multilevel optimization algorithms inspired by multigrid methods. More details on this method, and more examples of application can be found in [20] [2] .

The deformation field was chosen to be linear span-wise from root to tip ($n_k = 1$). Additionally, the leading and trailing edges, and the eight vertices of the bounding box were fixed throughout the optimization. Finally, only vertical displacements were considered for simplicity.

In a first experiment (see Figure 9), 6 control points at the root and at the tip were considered, for a total of 12 degrees of freedom.

In order to define an exercise in which the wing shape is optimized with respect to two disciplines, aerodynamics and structural design, that share a common set of design variables, the wing structure was treated as a thin shell which deforms under the load of aerodynamic forces. The distribution of stresses over the shell has been calculated by linear-elasticity, using a code of the public domain, ASTER developed by *Electricité de France (EDF).*

The four degrees of freedom located at mid-chord (at root and tip, over the upper and lower surfaces), marked S on Figure 9, were assigned to a player B (or S) in charge

of minimizing the following secondary criterion :

$$J_B = J_S = \iint_S \|\sigma.n\| \, dS + K_1 \max\left(0, 1 - \frac{V}{V_A}\right) + K_2 \max\left(0, \frac{S}{S_A} - 1\right) \tag{53}$$

in which σ is the stress tensor, S_A and V_A are the wing outer surface and volume at convergence of the purely-aerodynamic optimization, and K_1 and K_2 and penalty constants. By the reduction of this criterion, one expects a more uniform distribution of the load, and thus a more robust structure.

The remaining 8 degrees of freedom, marked A on Figure 9, were assigned to a player A in charge of minimizing the primary criterion, J_A.

It was possible to achieve a Nash equilibrium solution associated with the above split of the *primitive variables*, as indicated on Figure 10 which displays the convergence history of the aerodynamic and structural criteria. The sudden and occasional peaks correspond to iterations at which the constraint on lift is violated. The simplex method accommodates to this situation by discarding the point. Evidently, a stable Nash equilibrium is reached eventually.

Regrettably, this Nash-equilibrium configuration is totally unacceptable from a physical standpoint. The drag coefficient has doubled. The wing shape presents oscillations and the flow has been profoundly disrupted as indicated by the Mach number field (see Figure 11).

Besides, the number of iterations in this experiment may be found excessive. It should be pointed out that drag reduction problems are well known to be multimodal. They exhibit a *very large number of local minima*. Gradient-based methods are very cost efficient and useful in the final stage of convergence. But, if they converge in tens of iterations, in practice, they notably fail to provide a good estimate of the global optimum, unless the initial point is itself very close to it. Inversely, semi-stochastic methods, such as Genetic Algorithms, or Particle-Swarm optimizers, are far more robust, but often prohibitively expensive in aerodynamic optimum-shape design, due to the large number of flows required to be computed. For these reasons, for problems of intermediate difficulty, an acceptable compromise is often realized by the simplex method, which is deterministic,

but fairly robust. With this optimizer, the number of iterations, or computed flows governed by the compressible Euler equations in three dimensions, can be substantial, to achieve a satisfactory convergence on a nontrivial mesh, say, in hundreds, as in subsequent experiments (Figures 13 and 14). The even slower convergence in Figure 10 precisely reveals an inappropriate coupling. Nevertheless, since a typical 3D Eulerian-flow solution over a medium-size grid typically requires a few minutes of computation when using domain partitioning on a 32-cores Intel Xeon, this experiment can be realized in one day.

By this first experiment, we emphasize that even in case of convergence to a Nash equilibrium, the achieved configuration makes sense only if the split of variables is physically relevant.

In a second experiment, the number of design variables was reduced to 8 by considering a deformation field, only vertical and associated with the polynomial degrees $(3, 1, 1)$ along the longitudinal, vertical and span-wise directions. After a number of unsuccessful trials, a certain split of the primitive variables yielded acceptable results. The split corresponds to assign the 4 degrees of freedom at the root to player S $(=B)$ in charge of reducing the structural criterion, and the other 4, at the tip, to player A in charge of reducing the aerodynamic criterion (see Figure 12).

The convergence history of the two criteria in the dynamic game corresponding to this new split of design variables is indicated at Figure 13 a. The aerodynamic criterion is subject to numerous jumps due to the violation of the constraint on lift, but, as mentioned above, the simplex method accommodates to this. This phase of optimization is interrupted, somewhat arbitrarily after some 380 structural design steps; strictly speaking, convergence is not achieved, but the solution satisfactory since it realizes a visible improvement of the structural criterion of about 5 %, while the aerodynamic criterion has been increased of about the same percentage (only).

The cross sections at root, mid-span and wing tip corresponding to the initial and optimized shapes are represented on Figure 13 b, c and d. It appears that the structural control parameters tend to round out very slightly the root cross section for a better load distribution. This trend augments the drag, but here in proportions still acceptable,

because the process was interrupted after a variation of 5 % of each criterion. In fact, at this level of only partial convergence, the shape variations are still very small in amplitude because the coupling mechanism realized by the dynamic game is very stringent. Additionally, our *a priori* knowledge of the flow led us to locate the aerodynamic control parameters near the wing tip in the vicinity of the most sensitive region of the shock wave. Thus, this experiment does not reflect a blind split of variables, but instead one that was anticipated to be physically sound; and this was confirmed.

In the third experiment, the split of variables based on the proposed orthogonal decomposition of the restricted Hessian was implemented. Once the optimum of aerodynamics alone has been found at $\mathbf{y} = \mathbf{y}_A^\star$, a number of independent simulations corresponding to design vectors close to $\mathbf{y}_A^\star$ have been made to set up a database to model the behavior of the primary criterion J_A in terms of $\mathbf{y}$ by an RBF neural network [14] [22]. This meta-model was then used to approximate the gradient of C_D, the primary criterion to be minimized, the gradient of C_L, the constrained quantity, and the Hessian of C_D to form the restricted Hessian matrix. After diagonalization, the corresponding eigenvectors have been sorted by decreasing order of the associated eigenvalue, and split evenly in two subsets of four. Those associated with the four largest eigenvalues have been assigned to player A in charge of aerodynamics, and the remaining four to player S $(=B)$ in charge of reducing the criterion of structural design.

The proposed eigensplit led to a new dynamic Nash game, whose convergence history is indicated on Figure 14 a. The process was continued to a stage of convergence similar to previously in terms of coupling iterations. However, a notably superior performance was achieved : while the aerodynamic criterion was here only degraded of 3 %, the structural criterion was reduced of 8 %; equivalently, at equal stage of drag degradation, the improvement on the structural criterion is nearly three times larger. Note how the envelopes of the two curves are apparently initially tangent to the horizontal axis, a hint that in this formulation, the initial point is a robust design.

On Figure 14 b, c and d, the evolution of cross-sections at root, mid-chord and wing tip is indicated. It clearly appears from this figure that the shape variations are of larger

amplitude in this experiment than before, in the previous two experiments, but more distinctly located, as for example, on the lower surface of the wing at the root. Thus a wider operational territory for the secondary criterion is identified to cause a small and acceptable degradation only of the first criterion.

The split based on the orthogonal decomposition has permitted us to identify by a blind and automatic procedure, a set of structural parameters for which variations of larger amplitude, mostly visible on the lower surface of the wing, are possible without excessively affecting the shape in the critical region of the shock wave. Consequently, the principal characteristics of the flow are preserved, as indicated on Figure 15 which shows that the Mach number field has not been much altered from that obtained by pure aerodynamic optimization.

Thus, in conclusion, a significant reduction of 8 % of the structural criterion was realized while maintaining the flowfield configuration close to optimality (drag increase $< 3\,\%$), by an automatic procedure of orthogonal decomposition of the parameter space.

5 Application of territory splitting to other examples of two-discipline optimization

Since our original work on the aero-structural aircraft-wing optimum-shape design, we have applied the strategy of territory splitting in a Nash game to a number of cases of interest for aeronautics.

In Flight Mechanics, Niel [46] has used in-house explicit functional models incorporating the Bréguet laws in particular, to conduct multi-criterion aircraft performance analyses and optimizations, such as trade-offs between range and mass at take-off.

In the context of incompressible Navier-Stokes internal flow, F. Strauss [58] has applied successufully the same technique to minimize drag as primary objective, and maximize the real part of the second eigenvalue (for flow stabilty) as secondary objective.

In the next two sections, we summarize more actual numerical simulations of aeronautical interest that will be presented in full length elsewhere.

5.1 Sonic boom reduction

When an aircraft flies at supersonic speed, it generates a complex system of interacting waves in the near and far fields, as depicted in Figure 16. In particular, at ground level, generally an N-shaped pressure distribution is perceived, and it ought to be reduced for obvious environmental reason, while maintaining the aerodynamic performance of the aircraft. This leads to a classical two-objective design optimization problem in which the primary objective is drag ($J_A = C_D$, under the lift constraint: $C_L = 0.1$), calculated by a near-field CFD simulation, and the secondary objective is a measure of the sonic-boom intensity.

Our procedure has been presented in greater detail in [43] . The sonic boom at ground is evaluated using the three-layer approach [52]. After the near field has been calculated by CFD, the pressure is interpolated on a cylinder around the aircraft. The acoustic signal is then propagated through a non-uniform atmosphere using the acoustic ray-tracing code TRAPS [33] . The sum of the shock over-pressures of the under-track ground signature is then used as measure of the sonic boom intensity, J_B to be minimized as the the secondary objective function. This function can also be viewed as the total variation of the ground pressure, $J_B = TV(p_{\text{ground}})$.

To solve this two-objective optimization problem, the geometry of a generic supersonic configuration has been parameterized using ten geometrical design variables defined in Figure 17. In the subsequent Nash game, for simplicity only five of these parameters are retained for optimization: DV1, DV3, DV4, DV7 and DV8. The CFD calculation has been carried out using the ONERA *elsA* code [62] to solve the 3D Euler equations by upwind cell-centered finite volumes over a structured mesh using the Roe flux, and the Harten entropy correction. The number of elements varied from 350,000 to 500,000 according to mesh adaption, carried out a priori in the direction of shock wave propagation. The flight conditions have been $Z = 18,000$ m (altitude), $M_\infty = 1.6$ (Mach number), $\alpha = 2^o$ (AoA).

In our experiment, we have first optimized drag alone over the set of five parameters, and identified the absolute optimum. This optimization was carried out by the

evolutionary strategy CMA-ES [31] and simulations by the 3D Euler code.

Then, a database of aerodynamic coefficients (lift and drag) and acoustic impact (J_A and J_B) has been established by CFD simulations over a discrete set of design vectors $\mathbf{y}$ in the neighborhood of this optimum. Based on these data, meta-models $\tilde{J}_A$ and $\tilde{J}_B$ for J_A and J_B respectively, and for the lift constraint have been constructed. The minimum of $\tilde{J}_A$ (under lift meta-model constraint) was found for a slightly different design vector $\mathbf{y}_A^\star = (-0.558, -0.836, -0.506, -1.000, -0.434)$, used thereafter as initial design-point of the continuation procedure, developed according to the following steps:

1. Calculate an approximate reduced Hessian for $\tilde{J}_A$, and proceed to its diagonalization to identify the splitting matrix $\mathbf{\Omega}$. Thereafter, we have used:

$$\mathbf{\Omega} = \begin{bmatrix} \text{-0.1967} & \text{-0.1839} & \text{0.0944} & \text{-0.8251} & \text{-0.4876} \\ \text{-0.1257} & \text{-0.4079} & \text{-0.9042} & \text{0.0107} & \text{0.0114} \\ \text{-0.6606} & \text{-0.5744} & \text{0.3548} & \text{0.3282} & \text{-0.0037} \\ \text{-0.7055} & \text{0.6776} & \text{-0.2077} & \text{-0.0095} & \text{0.0049} \\ \text{0.1070} & \text{0.1036} & \text{-0.0672} & \text{0.4596} & \text{-0.8730} \end{bmatrix} \tag{54}$$

2. Increment the continuation parameter ϵ by step of 0.05, and for each fixed ϵ, organize the Nash game between the meta-models $\tilde{J}_A$ and $\tilde{J}_{AB}$. In this game, each objective function is optimized in a subspace about $\mathbf{y}_A^\star$. The objective-function $\tilde{J}_A$ is minimized by the SQP algorithm (see e.g. [28]) in the subspace spanned by the 2 eigenvectors associated with the largest two eigenvalues; these are the first two column-vectors of the above $\mathbf{\Omega}$ matrix. On the other hand, and possibly in parallel, the objective-function $\tilde{J}_{AB}$ is minimized by the Nelder-Mead simplex method [45] over the supplementary subspace of dimension 3. Both algorithms are applied to full convergence. Then the updated sub-vectors are exchanged, and ϵ is incremented.

3. The Nash-equilibrium design-points are evaluated *a posteriori* by high-fidelity CFD simulation, providing actual values for drag, J_A, and sonic-boom intensity, J_B. These are represented on Figure 18 by dotted lines.

The convergence history of the continuation process over the meta-models is indicated by solid lines in Figure 18. In complete conformity with the theory, the following points are observed:

1. For $\epsilon = 0$, all three curves initiate at the value 1, $\tilde{J}_A$ and $\tilde{J}_{AB}$ with zero slope. This is because $\bar{\mathbf{y}}_0 = \mathbf{y}_A^\star$, even though in the Nash game for $\epsilon = 0$, the trivial optimization of $\tilde{J}_A$ is not solved in the same space, but in a subspace of lower dimension, but the formulation has been devised to be consistent with the original optimum.

2. As ϵ increases the (meta-model) drag $\tilde{J}_A$ degrades monotonically, while the objective function $\tilde{J}_{AB}$ diminishes; the secondary objective function $\tilde{J}_B$, despite nonlinear effects, also decreases monotonically in this experiment.

3. It is the designer's option to decide which level of degradation of $\tilde{J}_A$ is acceptable to improve $\tilde{J}_B$. This decision is more sensibly made on the actual high-fidelity evaluation rather than through meta-models.

The *a posteriori* CFD simulation of the Nash-equilibrium design-points (dotted lines in Figure 18) confirms that using a Nash game combined with a strategy of territory-splitting results in a configuration with a reduced boom impact at ground, J_B, almost preserving the aerodynamic optimum performance, J_A. The slight discrepancy, at $\epsilon = 0$, between the actual drag, J_A, and the corresponding meta-model value, $\tilde{J}_A$, is not related to the Nash game formulation. It is due to the fact that in this experiment, the meta-model was not constructed (or corrected) prior to the Nash game to achieve its minimum at exactly the same design-point $\mathbf{y}_A^\star$ as the physical model. Nevertheless, for example with $\epsilon = 0.6$, the actual drag is increased of nearly 4%, while the sonic-boom intensity is reduced of some 8%, thus demonstrating the potential of the formulation.

5.2 Helicopter rotor blade optimization in hover and forward motion configurations

The two-point aerodynamic shape optimization of a helicopter rotor blade was presented in greater detail in [50] . Here we present a typical illustration of the Nash game strategy

that is employed to carry on this on-going optimization campaign.

The principal discipline to be optimized is the performance in hover, measured by the Figure of Merit. The secondary discipline is the performance in forward flight, estimated by the rotor required power. The blade shape has been parameterized using a span-wise Bézier discretization defining deformation laws of twist, sweep, chord and anhedral. Therefore, the design variables were the values of the Bézier poles, defined as deformations with respect to the initial blade planform.

The baseline rotor used throughout the computations has been the ERATO rotor (Figure 19, left). This model rotor, developed in a joint program between Eurocopter, ONERA and DLR was devised to reduce noise emissions [49] . It features a 2.1m radius, a mean chord of 0.14m and a linear twist of -10/R. The blade planform has forward and backward sweep as well as a non-optimized straight tip.

In the hover simulations, the collective pitch was used as an additional design variable in order to achieve the maximum Figure of Merit, for all lift coefficients. In forward flight computations, the rotor was trimmed imposing zero flapping (i.e. $\beta_{lc} = \beta_{ls} = 0$). Other conditions are the following: $Z_b = 12.5$ (thrust coefficient), $CxS = 0.1$ (propulsive to drag force ratio), tip Mach number $M_{\text{tip}} = 0.617$, and forward motion parameter $\mu = M_\infty / M_{\text{tip}} = 0.344$ corresponding to a forward speed of 260 km/h. This gives a tip Reynolds number of 1.93 Million (based on average chord and tip velocity).

The first step of the algorithm consists in the single-objective optimization of the rotor blade shape in hover flight alone (primary discipline). The flow computations were performed by the solution of the 3D Reynolds-Averaged Navier-Stokes (RANS) equations over a single-block mesh of 0.81 million points for a quarter-blade geometry (Figure 19 right). The optimization of the baseline rotor was performed using Dakota, an open-source optimizing tool developed by Sandia Laboratories containing multiple optimization algorithms [3] . Among the available algorithms CONMIN, a gradient-based method, was used since the *elsA* adjoint solver delivers the computation of gradients at a minimal cost.

The hover optimizations using the adjoint *elsA* simulations show the classical trends (as well-documented in [21]) , namely an increase of the twist and the chord at the blade

tip and a decrease of the forward and backward sweep of the original blade. An increase of approximately 5 to 7 Figure of Merit points has been achieved.

This reference point being established, and given the very large computational cost of evaluating the hover rotor performance with high fidelity codes, the subsequent two-point optimization was performed using meta-models.

A Kriging surrogate model of the hover objective function (Figure of Merit) was built using a database of CFD computations near the hover optimum. Technically $J_A = 100(1 - FM)$. This surrogate model was then used to estimate the Hessian value at the optimum (and hence the appropriate variable territory split) as well as to evaluate the objective function in the subsequent optimizations.

The secondary discipline, i.e. the required power for forward motion (J_B), was evaluated using Eurocopter's code HOST (*Helicopter Overall Simulation Tool* [12]). This is a rotor comprehensive code that considers the blade dynamics, using a 1D Euler-Bernouilli beam model, coupled with a simplified aerodynamics model based on lifting-line theory.

Equipped with a meta-model for the primary discipline, and a low-fidelity model for the secondary discipline, in the second step of the optimization process, a number of Nash game simulations between these two models were launched using FAMOSA (*Full and Adaptive Multi-Level Optimum Shape Algorithm* [23]) , an in-house toolbox for optimization.

Sixteen primitive variables were used (5 poles for twist-angle, 5 poles for chord variation, 5 poles for sweep variation, and collective pitch). These have been split according to the Hessian eigen-decomposition in preparation of the Nash game, the continuation parameter ϵ was incremented by steps of 1/10. For each ϵ, typically 3 coordination iterations were performed before exchange of variables between players. Figure 20 illustrates the convergence history of a typical Nash game process.

Again, the consistency of the Nash game with the single-primary-discipline optimization is demonstrated when the design variables are split appropriately.

The pay-off to be consented on hover-motion performance to achieve a reduction in the requires power for forward motion is established in the case of this experiment.

In this section and the previous ones, we have considered applications of Nash games as strategies to identify viable trade-offs between antagonistic concurrent disciplines. In the next section, we introduce *virtual* Nash games in which players cooperate in the optimization of the same objective function.

6 Cooperative design with local / global parameters by virtual Nash games

6.1 Design problem description

Previous sections demonstrated how Nash games can be used to determine an equilibrium between two antagonistic criteria. Nevertheless, this approach can also be employed in a collaborative framework, if all players aim at optimizing the same objective. In this context, the splitting of territory becomes a domain decomposition which could accelerate the convergence and help avoiding local optima. This approach was proposed by Périaux [48]. As illustration, we consider a wing design problem, which requires the definition of global geometrical characteristics, such as span, root/tip length ratio, angle of attack, twist angle, sweep angle, etc, as well as local geometrical features that determine the wing section. The single design objective considered for this study is the drag minimization, under a lift constraint, the flow being modeled by the three-dimensional compressible Euler equations. In this context, Nash games are used now to find a better solution, in terms of global and local parameters, than the one found by a classical optimization.

The design optimization problem consists in minimizing the drag coefficient, here augmented by a penalty term on the lift coefficient. Both coefficients are viewed as functions of the N-dimensional design vector Y:

$$J(\mathbf{y}) = C_D + \rho \max(0\,; C_L^{ref} - C_L), \tag{55}$$

where ρ is a penalty parameter to be calibrated and C_L^{ref} the reference lift coefficient (in the subsequent experiment: $\rho = 10^4$). The choice of the parameters $Y = (\mathbf{y}_i)_{i=1,\dots,N}$ that

defines the wing shape can be done in several ways, which depend on the context. In this study, we would like to optimize *global*, as well as *local* wing characteristics. The baseline of the wing is described in[5] . The global characteristics of the wing shape are obtained from five parameters : the span, the root / tip chord length ratio, the angle of attack, the twist angle and the sweep angle, as shown in Figure 21. The local characteristics of the wing shape are defined by imposing the section shape, which is constructed thanks to two cubic B-Spline curves, one for the suction side and one for the pressure side. Thus, the section shape is determined by 2×5 control points, which can be moved in crosswise direction. Control points located at leading edge and trailing edge are kept fixed. The section shape is the same for the whole wing.

6.2 Single optimization exercises

An optimization is achieved for three independent numerical experiments, involving only local shape parameters, only global shape parameters, and finally local and global shape parameters. Therefore, the number of optimization variables is successively $N = 10$, $N = 5$ and $N = 15$. For each new set of parameters provided by the optimizer, the wing shape is constructed automatically. When local shape parameters are optimized, global shape parameters are set according to the baseline wing shape, and vice versa. An unstructured grid, that counts approximatively 200 000 nodes, is then build for each new geometry using the GMSH grid generation software [27]. The state equations are then solved using the NUM3SIS in-house parallel simulation platform [36]. The Covariance Matrix Adaption Evolution Strategy (CMA-ES) algorithm [32], which is known for its robustness, is employed.

The evolution of the cost function, for the three experiments performed, is plotted in Figure 22. As can be seen, local shape optimization is very effective in this context, because a local shape change can reduce significantly the shock wave on the suction side of the wing. Figures 23 and 24 illustrate the modification of the pressure field. The optimization of global parameters yields a more limited drag reduction. When considering the pressure field plotted in Figure 25, one can observe that the global shape change

cannot reduce significantly the shock wave. However, the optimizer finds a solution that reduces the impact of the shock wave on the drag value. The result obtained by optimizing simultaneously local and global parameters is unexpected: the drag reduction is slightly better than that obtained with only global shape change, but far worse than that obtained with only local shape optimization. A better result was expected, since the design space generated by local shape change is included in the design space generated by local and global shape modifications. The observation of pressure field in Figure 26 shows that the optimizer has modified global and local shape parameters slightly, yielding a poor result. One may suppose that the mixing of global and local parameters leads to an optimization problem that exhibits several local minima, in which the optimizer is trapped.

6.3 Nested and successive optimizations

Since a straightforward optimization including local and global shape parameters fails, we consider other strategies. At first, we try a nested approach, that consists of two phases: in a first phase, only global shape parameters are optimized, yielding the global characteristics of the wing. This design is then considered as a starting point for the second phase, during which local and global parameters are optimized. Actually, the first phase is just used to modify the initial point for the optimizer. We hope this can help to avoid being trapped in local minima.

The results obtained by carrying out this strategy can be shown in Figure 27. Starting from the design optimized with respect to global shape parameters leads to a better cost function value. However, this result is not better than that obtained using only local parameter changes. Moreover, the computational cost is significantly increased. This experiment shows that the design obtained by the optimization of global parameters is not a satisfactory starting point for the optimization of global and local parameters.

A common practice in engineering design consists of optimizing successively global and local shape parameters. With such an approach, a first step aims at determining suitable global shape characteristics, whereas the second step modifies the shape obtained by local perturbations. This approach can be successful if the optimization problem is

characterized by a so-called *separability* property. It means that the optimum can be reached by successive modifications of design variables. This approach is thus tested, by optimizing the local shape parameters, after the global shape parameters have been optimized. Results are shown Figure 28. As can be seen, the cost function value reached is slightly better than the one obtained by a single optimization of local parameters. Moreover, this result is better than those obtained in previous experiments with local and global parameters. This surprising result shows that optimizing separately local and global parameters is far more efficient than considering these variables as a whole.

6.4 Virtual game strategy

The previous experiment suggests the use of virtual Nash games, as a way to couple the optimizations of local and global shape parameters. Indeed, Nash games are based on the concept of *split of territories*, that consists in splitting the design variables in two sets, each set being optimized independently by a so-called *player*. In this case, both players tend to improve the same cost function, and for this reason, we refer to such a formulation as a *virtual* Nash game. In the context of local and global shape parameterization, the two sets naturally correspond to the local $\mathbf{y}_L$ and global $\mathbf{y}_G$ parameter sets.

The algorithm employed is a special case of the algorithm in Section 1:

1. choose a global/local split of territory $\mathbf{y} = (\mathbf{y}_G, \mathbf{y}_L)$
2. choose initial design variables $\mathbf{y}^{(0)} = (\mathbf{y}_G^{(0)}, \mathbf{y}_L^{(0)})$;
   $k \leftarrow 0$;
3. begin game-loop iteration k;
4. carry out in parallel respectively K_G, K_L optimization iterations by two players :
   - first player updates $\mathbf{y}_G^{(k)}$ to $\mathbf{y}_G^{(k+1)}$ with fixed $\mathbf{y}_L = \mathbf{y}_L^{(k)}$;
   - second player updates $\mathbf{y}_L^{(k)}$ to $\mathbf{y}_L^{(k+1)}$ with fixed $\mathbf{y}_G = \mathbf{y}_G^{(k)}$;
5. synchronize the players : $\mathbf{y}^{(k+1)} = (\mathbf{y}_G^{(k+1)}, \mathbf{y}_L^{(k+1)})$

6. end game-loop iteration k;

   if a stopping criterion is reached then STOP ;

   else $k \leftarrow k+1$ GOTO step (2).

Such a strategy can reduce significantly the computational cost because each optimization is carried out in a design space of lower dimension and they can be solved in parallel, since they are independent. The above-described algorithm is carried out using only three iterations of the optimizer for each update achieved by the two players. The evolution of the cost function is indicated in Figure 29. Evidently, a significantly improved solution is obtained at a computational cost similar to a single optimization over the full parameter space.

We compare the local and global shape parameters in tables 2 and 3, for the initial wing and wings obtained by single optimizations and game strategy. Obviously, the single optimization of global parameters and the game strategy yield shape modifications of opposite sign (except for the sweep angle). On the contrary, some similarities can be observed when comparing the shapes obtained using single optimization of local parameters and game strategy. This shows that the coupling of local and global parameters optimization modifies strongly the global parameters, but only slightly the local ones. A comparison of the shapes and the pressure fields, for the initial wing and the wing optimized by Nash game, is depicted in Figure 30.

design variable	initial	global optimization	Nash game
span	2.59	2.49	2.75
root/tip ratio	0.3631	0.297	0.403
angle of attack	2.	2.272	1.899
twist angle	-1.	-0.775	-1.176
sweep angle	76.76	68.92	69.84

Table 2: Comparison of optimized global parameters.

Finally, this study demonstrates that Nash games can also be employed successfully as a domain decomposition method, in order to speed-up the convergence and avoid being trapped by local optima.

design variable	initial	local optimization	Nash game
$\mathbf{y}_1^s$	2	2.27	2.61
$\mathbf{y}_2^s$	5	3.95	4.17
$\mathbf{y}_3^s$	6	4.92	5.31
$\mathbf{y}_4^s$	4	4.74	4.29
$\mathbf{y}_5^s$	2	2.30	2.07
$\mathbf{y}_1^p$	-2	-2.02	-1.67
$\mathbf{y}_2^p$	-5	-4.47	-4.82
$\mathbf{y}_3^p$	-6	-6.06	-5.36
$\mathbf{y}_4^p$	-4	-4.04	-3.90
$\mathbf{y}_5^p$	-2	-2.12	-1.82

Table 3: Comparison of optimized local parameters.

7 Conclusions

High-fidelity models are today more routinely solved by advanced simulation platforms in the analysis of complex engineering systems. This offers computational specialists a great challenge to include such PDE simulations in the design optimization loop. The most relevant optimization approaches are multi-objective, and even multi-disciplinary in nature. In this context, Nash games offer a versatile formalism to handle the corresponding coupling between different simulation and optimization tools that share a common set of design variables, and are well-adapted to parallel computing.

In certain rather simple physical situations involving only a few design variables, whose influence on the various objective functions is at least qualitatively known a priori, it is sometimes possible to identify a natural split of the primitive design variables yielding a sensible Nash equilibrium. We have provided two such examples: the inverse design of an airfoil with respect to lift and drag, and the structural-thermal optimization of a plate.

However, optimum-shape design of 3D geometries in compressible aerodynamics provides an example of a situation that is more complex in at least two respects. One is that it is usually difficult to identify a priori the influence of the geometrical variables individually. Second, transonic flows are fragile solutions, since the delicate shape optimization in the shock region is essential to maintain sub-optimality. In such situations, we advocate defining the split of design variables, or split of territory in our terminology, based on an eigen-decomposition of the design space.

Thus, a theoretical formulation has been proposed for situations of this type, permitting to identify a sub-optimal solution as a Nash-equilibrium solution between virtual players in charge of reducing two independent criteria. An orthogonal decomposition of the design space is made to assign the player in charge of the secondary criterion a subspace of action, or territory, in which the primary criterion has little sensitivity.

The method has been tested first over a simplified test-case of aero-structural shape optimization of a business jet wing combining drag reduction under lift constraint in a transonic cruise configuration with the reduction of an integral of the stress over the structure. In this example, after a first phase of purely aerodynamic optimization, the primary criterion (drag) was modeled at convergence by an RBF neural network in order to approximate gradients and Hessians necessary to the construction of the orthogonal basis. This basis was then used as the support of a dynamic Nash game in a novel formulation. The numerical experiments have clearly demonstrated the superiority of concurrent optimizations realized using the orthogonal decomposition as a support, in terms of asymptotic convergence stability, and achieved performance as well.

This approach has more recently been applied with similar success to the shape optimization of a generic supersonic aircraft with respect to drag and sonic-boom reduction, and to the shape optimization of a helicopter rotor blade with respect to performance in both hover and forward motion configurations.

Lastly, we have given an example of a virtual Nash game formulation used as a partitioning technique to gain computational efficiency.

As a final remark, we note that the above Nash games have been introduced to handle the antagonism between conflicting disciplines, when a discipline is preponderant or fragile. In this sense, these are competitive algorithms. When instead all disciplines have comparable importance, it is possible to generalize the classical steepest-descent method by defining a direction of search for which the directional derivatives of all objective functions are of the same sign, or even equal. This results in a cooperative algorithm, *Multiple-Gradient Descent Algorithm (MGDA)* [18] [19] .

Acknowledgments

Nash games were introduced to the authors by the late J.-L. Lions, and J. Périaux, as methods particularly well-suited for decentralized computation by decomposition methods such as domain partitioning via optimal control formulations. Their scientific insight has been a great source of inspiration.

The numerical demonstrations in this article have been to great extent devised and realized by our collaborators, whose contribution has been essential: N. Marco performed our earliest Pareto set identification by NSGA, Z.L. Tang (NUAA, P.R. China) inspired the two-point aerodynamic airfoil optimization, M. Thellner (Linköping University, Sweeden) led the topology optimization experiment on the structural-heat system, B. Abou El Majd (Aïn Chock Casablanca University, Morocco) carried out the aero-structural wing-shape optimization by adaptive splitting; more recently A. Minelli (ONERA/DAAP, France) and E. Roca León (ONERA/DAAP and Eurocopter) extended this approach to the aero-bang optimization of the supersonic aircraft and the rotor blade optimization respectively.

References

[1] Abou El Majd, B.: Algorithmes hiérarchiques et stratégies de jeux pour l'optimisation multidisciplinaire – Application à l'optimisation de la voilure d'un avion d'affaires. Ph.D. thesis, Université de Nice-Sophia Antipolis (2007). http://tel.archives-ouvertes.fr/tel-00529309/fr/

[2] Abou El Majd, B., Désidéri, J.-A., Duvigneau, R.: Shape design in Aerodynamics: parameterization and sensitivity, vol. 17 (1-2), chap. Multilevel Strategies for Parametric Shape Optimization in Aerodynamics. Revue Européenne de Mécanique Numérique European Journal of Computational Mechanics (2008).

[3] Adams, B.M.: *The Dakota Toolkit for Parallel Optimization and Uncertainty Analysis.* SIAM Conference on Optimization, Boston, MA, May (2008).

[4] Alexandrov, N.M.: Comparative properties of collaborative optimization and other approaches to mdo. Tech. rep., ICASE, Hampton, VA (1999).

[5] Andreoli, M., Janka, A., Désidéri, J.-A.: Free-Form Deformation parameterization for multilevel 3D shape optimization in aerodynamics, INRIA Research Report 5019 (2003).

[6] Attouch, H., Redont, P., Soubeyran, A.: A new class of alternating proximal minimization algorithms with costs-to-move. SIAM J. Optim. **18**(3), 1061–1081 (2007).

[7] Aubin, J.-P.: *Mathematical methods of game and economic theory.* - Amsterdam, New York. North-Holland Publishing Co.(1979).

[8] Auroux, D., Clément, J., Hermetz, J., Masmoudi, M., Parte, Y.: Multidisciplinary Design Optimization in Computational Mechanics, chap. Collaborative Optimization. Wiley/ISTE (2010), P. Breitkopf and R. Filomeno Coelho Eds.

[9] Basar, T., Olsder, G.J.: Dynamic Noncooperative Game Theory. Academic, Bodmin, Cornwall, Great Britain (1995).

[10] Bendsøe, M.P.: Optimization of Structural Topology, Shape, and Material Springer-Verlag, Berlin (1995).

[11] Bendsøe, M.P., Sigmund, O.: Material interpolation schemes in topology optimization, Arch. Mech. 69, 635–654 (1999).

[12] Benoit, B., Dequin, A.M., Kampa, K., Von Grnhagen, W., Basset, P.M., Gimonet, B.: *Host, a General Helicopter Simulation Tool for Germany and France.* American Helicopter Society 56th Annual Forum Proceedings, Virginia Beach, USA, May (2000).

[13] Bruns, T.E., Tortorelli, D.A.: Topology optimization of nonlinear elastic structures and compliant mechanisms, Comput. Methods Appl. Mech. Engg. 190, 3443-3459 (2001).

[14] Chandrashekarappa, P., Duvigneau, R.: Radial basis functions and kriging metamodels for aerodynamic optimization. Research Report 6151, INRIA (2007).

[15] Ciarlet, P.G.: The Finite Element Method for Elliptic Problems North Holland, Amsterdam (1978).

[16] Désidéri, J.-A.: Split of Territories in Concurrent Optimization. Research Report 6108, version 6, INRIA (2007). URL: https://hal.inria.fr/inria-00127194

[17] Désidéri, J.-A.: Cooperation and competition in multidisciplinary optimization - Application to the aero-structural aircraft wing shape optimization. *Computational Optimization and Applications*, 52 (1), 29-68 (2012).

[18] Désidéri, J.-A.: Multiple-Gradient Descent Algorithm (MGDA). Research Report 6953, INRIA (2009). *URL:* http://hal.inria.fr/inria-00389811/fr/

[19] Désidéri, J.-A.: Multiple-gradient descent algorithm (MGDA) for multiobjective optimization. *Comptes Rendus de l'Académie des Sciences Paris*, 350:313–318, 2012.

[20] Désidéri, J.-A., Abou El Majd, B., Janka, A.: Nested and Self-Adaptive Bézier Parameterizations for Shape Optimization. J. Comput. Phys. **124**(1), 117–131 (2007).

[21] Dumont, A., Le Pape, A., Peter, J., Huberson, S.: *Aerodynamic Shape Optimization of Hovering Rotors Using a Discrete Adjoint of the RANS Equations".* Journal of the American Helicopter Society, Volume 56, Number 3, pp. 1-11, July (2011).

[22] Duvigneau, R.: Meta-Modeling for Robust Design and Multi-Level Optimization. In: 42e Colloque d'Aérodynamique Appliquée, Couplages et Optimisation Multidisciplinaires, INRIA Sophia Antipolis, 19-21 March (2007).

[23] Duvigneau R., Kloczko T., and Praveen C.: *A three-level parallelization strategy for robust design in aerodynamics.* 20th International Conference on Parallel Computational Fluid Dynamics Proceedings, Lyon, France, May (2008).

[24] Ekeland, I., Temam, R.: Convex Analysis and Variational Problems North-Holland Publishing Company (1976).

[25] Eschenauer, H.A., Olhoff, N.: Topology optimization of continuum structures: A review, Appl. Mech. Rev. 54, 331-390 (2001).

[26] Fonseca, C., Fleming, P.: Multiobjective optimization and multiple constraint handling with evolutionary algorithms. I A unified formulation. In: Transactions on Systems, Man and Cybernetics, Part A, 28(1), 26-37. IEEE (1998).

[27] Geuzaine, C., Remacle, J.-F.: GMSH: a three-dimensional finite element mesh generator with built-in pre- and post-processing facilities, Int. J. for Numerical Methods in Fluids 79 (2009).

[28] Gill, P.E., Murray, W., and Wright, M.H.: Practical Optimization. Academic Press, London (1986).

[29] Goldberg, D.: Genetic Algorithms in Search, Optimization and Machine Learning. Addison Wesley Company Inc. (1989).

[30] Habbal, A., Thellner, M., Petersson, J.: Multidisciplinary topology optimization solved as a Nash game. J. Numer. Meth. Engg. **61**(7), 949–963 (2004).

[31] Hansen, N., Ostermeier, A.: Completely derandomized self-adaptation in evolution strategies, Evolutionary Computation **9**(2), 159–195 (2001).

[32] Hansen, N., Muller, S.D., Koumoutsakos, P.: Reducing the Time Complexity of the Derandomized Evolution Strategy with Covariance Matrix Adaptation, Evolutionary Computation **11**(1), 1-18 (2003).

[33] Hayes W.D., Haefeli R.C. and Kulsrud H.E.: Sonic Boom Propagation in a Stratified Atmosphere with Computer Program. *NASA CR-1299* (1969).

[34] Horn, J., Nafpliotis, N., Goldberg, D.E.: A Niched Pareto Genetic Algorithm for Multiobjective Optimization. In: Proc. of the First IEEE Conference on Evolutionary Computation, IEEE World Congress on Computational Intelligence (ICEC'94), **1**, 82-87. Piscataway, NJ: IEEE Service Center (1994).

[35] Keane, A.J., Nair, P.B.: Computational Approaches for Aerospace Design, The Pursuit of Excellence. John Wiley & Sons, Ltd, Chichester, England (2005).

[36] Kloczko, T.: Concept, architecture and performance study for a parallel code in CFD, Parallel CFD Conference, Lyon, France (2008).

[37] Knowles, J. D., Corne, D.W.: Approximating the Nondominated Front Using the Pareto Archived Evolution Strategy. MIT Press Journals, Evolutionary Computation, **8**(2), 149-172 (2000).

[38] Leoviriyakit, K., Jameson, A.: Case studies in aero-structural wing planform and section optimization. In: 22nd Applied Aerodynamics Conference and Exhibit. Providence, Rhode Island (2004).

[39] Marcelet, M.: Etude et mise en œuvre d'une méthode d'optimisation de forme couplant simulation numérique en aérodynamique et en calcul de structure. Ph.D. thesis, Ecole Nationale d'Arts et Métiers, Paris (2008).

[40] Marco, N., Désidéri, J.-A., Lanteri, S.: Multi-Objective Optimization in CFD by Genetic Algorithms. Tech. Rep. 3686, INRIA (1999).

[41] Marco, N., Lanteri, S., Désidéri, J.-A., Mantel, B., Périaux, J.: A parallelized genetic algorithm for a 2-D shape optimum design problem. Surveys on Mathematics for Industry **9**, 207–221 (2000).

[42] Miettinen, K.: Nonlinear Multiobjective Optimization. Kluwer Academic Publishers, Boston/London/Dordrecht (1999).

[43] Minelli, A, Salah El Din, I., Carrier, G., Zerbinati, A., Désidéri, J.-A..: Cooperation and Competition Strategies in Multi-Objective Optimization, Application to a Low-Boom/Low-Drag Supersonic Business Jet. AIAA Applied Aerodynamics Conference, San Diego, California , 24-27 June (2013).

[44] Nash, J.F.: Non-Cooperative Games. Annals of Mathematics **54**(2), 286–295 (1951).

[45] Nelder, J.A., Mead, R.: A Simplex Method for Function Minimization. Computer Journal **7**, 308–313 (1965).

[46] Niel, J.: Multicriterion aircraft performance optimization using explicit functional models. M.E. report, University of Nice (2008).

[47] Périaux, J., Chen, H.Q., Mantel, B., Sefrioui, M., Sui, H.T.: Combining game theory and genetic algorithms with application to DDM-nozzle optimization problems. Finite Elem. Anal. Des., **37**(5), 417-429 (2001).

[48] Périaux, J., Lee, D.S., Gonzales, L.F., Srinivas, K.: Fast reconstruction of aerodynamic shapes using evolutionary algorithms and virtual Nash strategies in a CFD design environment, Journal of Computational and Applied Mathematics 232 (2009).

[49] Prieur, J., Splettstoesser, W.R.: *ERATO - An ONERA-DLR Cooperative Programme On Aeroacoustic Rotor Optimization.* 25th European Rotorcraft Forum, Rome, Italy, September (1999).

[50] Roca Léon, E., Le Pape, A., Désidéri, J.-A., Alfano, D., Costes, M.: Concurrent Aerodynamic Optimization of Rotor Blades Using a Nash Game Method: 69th American Helicopter Society Forum, , Phoenix, Arizona, 21-23 May (2013).

[51] Rodrigues, H., Fernandes, P.: A material based model for topology optimization of thermoelastic structures, Int. J. Num. Meth. Engg., **38**, 1951-1965 (1995).

[52] Salah-el-Din, I., Le-Pape, M.C., Minelli, A., Grenon, R., Carrier, G.: Impact of Multipole Matching Resolution on Supersonic Aircraft Sonic Boom Assessment. 4th Eucass, St. Petersbourg (2011).

[53] Samareh, J.A.: Multidisciplinary Aerodynamic-Structural Shape Optimization Using Deformation (MASSOUD). AIAA 2000-4911. In: 8th AIAA/NASA/USAF/ISS, MO Symposium on Multidisciplinary Analysis and Optimization, September 6-8, 2000/Long Beach, CA (2000).

[54] Sigmund, O.: Design of multiphysics actuators using topology optimization Part I: One-material structures, Comp. Meth. Appl. Mech. Engg. (2001).

[55] Sobieszczanski, J., Haftka, R.T.: Multidisciplinary aerospace design optimization: survey of recent developments. Structural Optimization **14**, 1–23 (1997).

[56] Sobieszczanski-Sobieski, J., Altus, T., Sandusky, R.R.: Bilevel integrated system synthesis for concurrent and distributed processing. AIAA J. **41**(10), 1996–2003 (2003).

[57] Srinivas, N., Deb, K.: Multi-objective function optimization using non-dominated sorting genetic algorithms. Evolutionary Computation **2**(3), 221-248 (1995).

[58] Strauss, F., Désideri, J.-A., Duvigneau, R., Heuveline, V.: Multiobjective optimization in hydrodynamic stability control. Research Report No. 6608, INRIA (2008). *URL:* http://hal.inria.fr/inria-00309693

[59] Svanberg, K.: The method of moving asymptotes - a new method for structural optimization, Int. J. Numer. Methods Engg., **24**, 359-373 (1987).

[60] Tang, Z., Désidéri, J.-A., Périaux, J.: Multi-criterion aerodynamic shape-design optimization and inverse problems using control theory and Nash games. Journal of Optimization Theory and Applications **135**(1) (2007).

[61] Tedford, N.P., Martins, J.R.R.A.: Comparison of MDO architectures within a universal framework. AIAA 2006-1617. In: 47th AIAA/ASME/ASCE/AHS/ASC Structures, Structural Dynamics, and Materials Conference. Newport, Rhode Island (2006).

[62] Veuillot, J.-P., Cambier, L.: Status of the *elsA* CFD Software for Flow Simulation and Multidisciplinary Applications. AIAA 2008-664 (2008).

[63] Wang, J.: Optimisation Distribuée Multicritère par Algorithmes Génétiques et Théorie des Jeux & Application à la Simulation Numérique de Problèmes d'Hypersustentation en Aérodynamique. Ph.D. thesis, University of Paris 6 (2001). Spéc.: Math. App.

[64] Zitzler, E., Thiele, L.: An evolutionary algorithm for multiobjective optimization: The strength Pareto approach. Tech. Rep. 43, Computer Engineering and Networks Laboratory (TIK), Swiss Federal Institute of Technology (ETH) Zurich, Gloriastrasse 35, CH-8092 Zurich, Switzerland (1998).

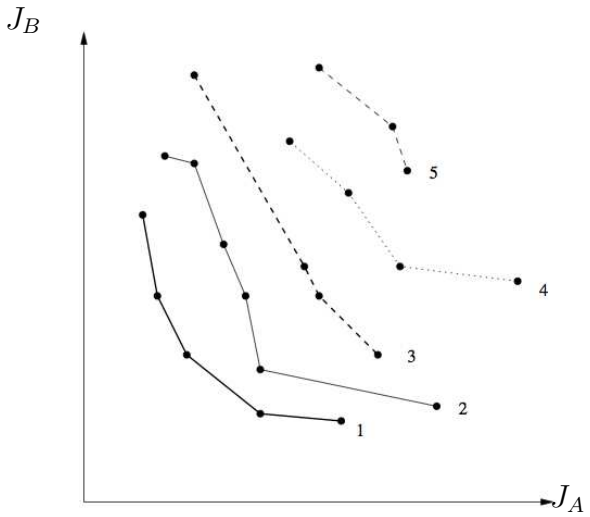

Figure 1: Sketch of a population of design-points sorted in Pareto fronts

a) Accumulated design-points in function space
(⋄ : fine grid; + coarse grid)

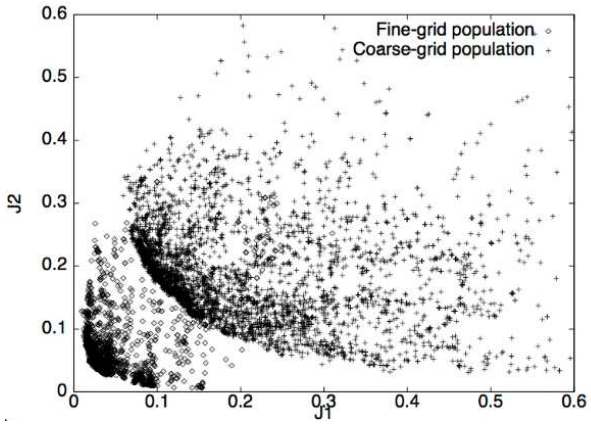

b) Discrete Pareto fronts
(⋄ : fine grid; + coarse grid)

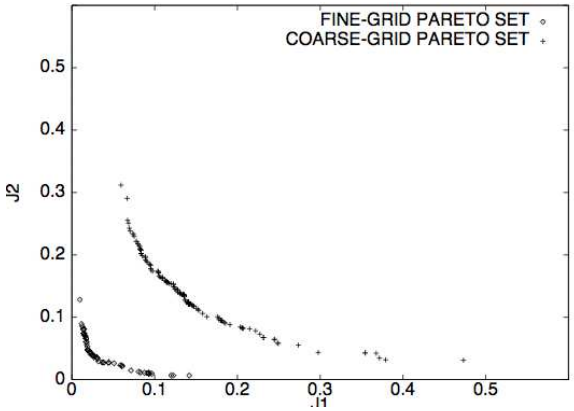

c) Shapes associated with the (fine-grid) Pareto-optimal solutions

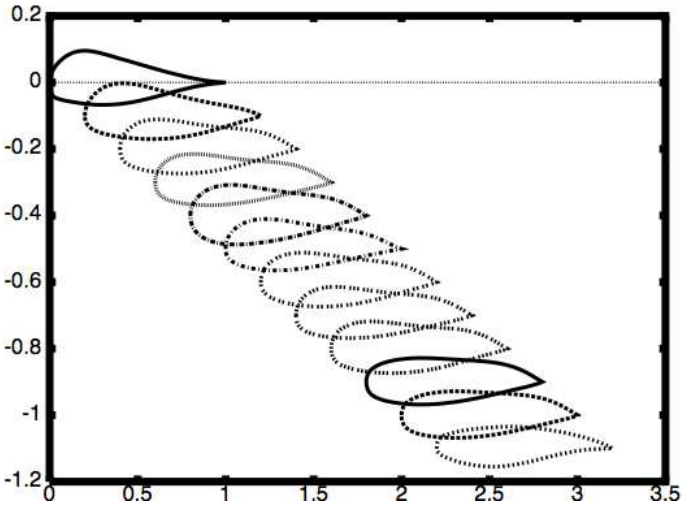

Figure 2: An illustration of the NSGA in which an airfoil shape is optimized to reduce drag and maximize lift concurrently through Eulerian flow simulations; in c) the upper-left airfoil has the highest lift, and the lower-right the lowest drag.

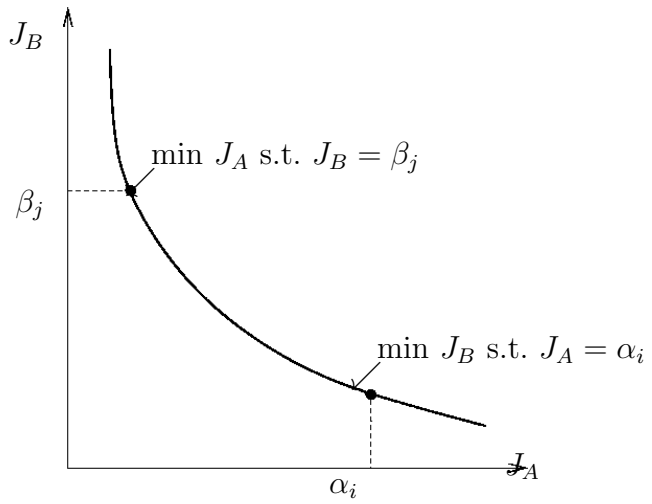

Figure 3: Schematic of a Pareto front point-wise identification by the treatment of certain criteria as equality constraints

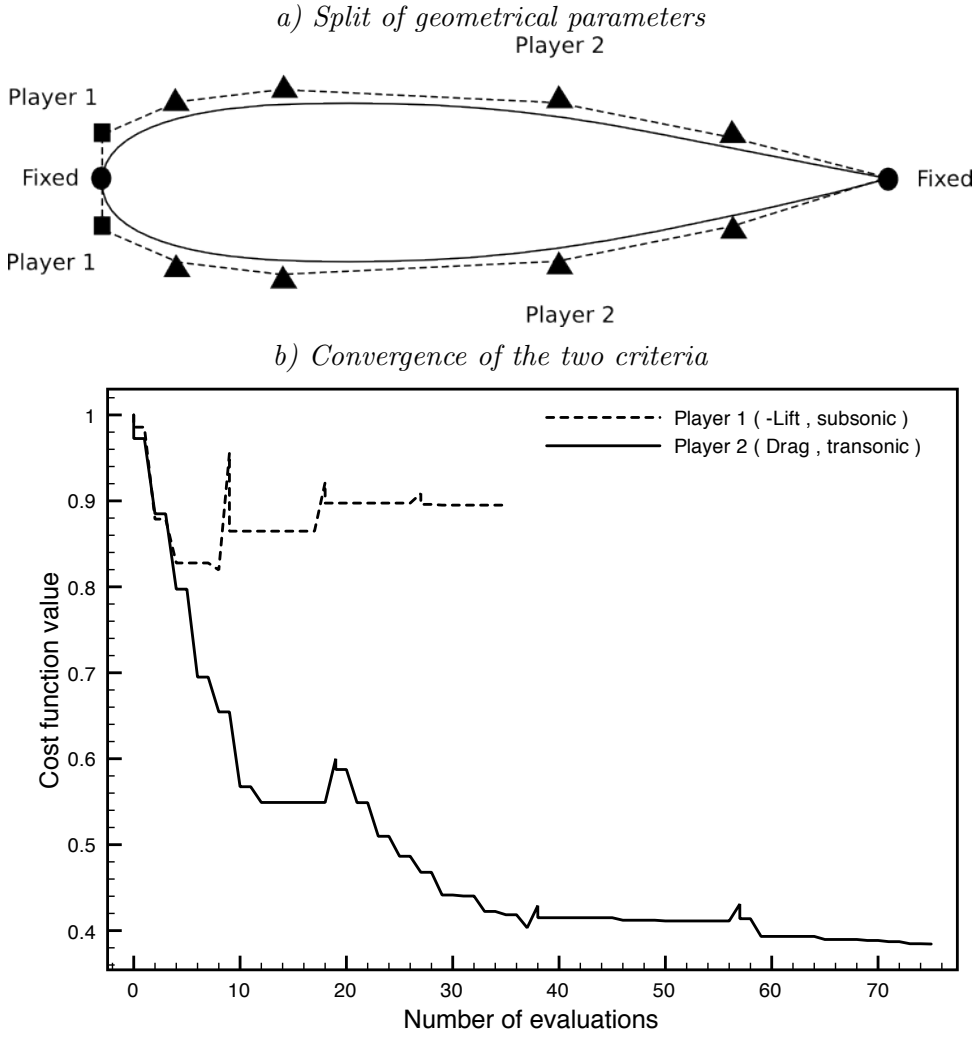

Figure 4: Split of territory and optimization strategy; information exchange every 5 ‖ 10 parallel optimization iterations between player 1 (squared control points) and player 2 (triangular control points)(top); asymptotic convergence of the two criteria towards a Nash equilibrium (bottom).

a) Subsonic case (lift enhanced by player 1)

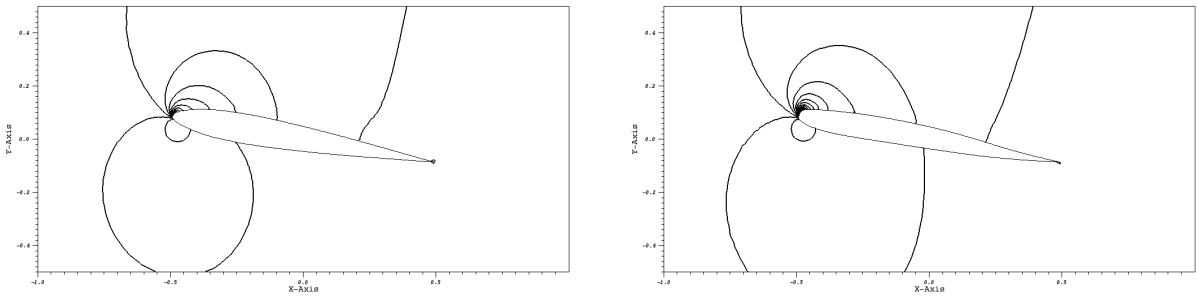

b) Transonic case (drag reduced by player 2)

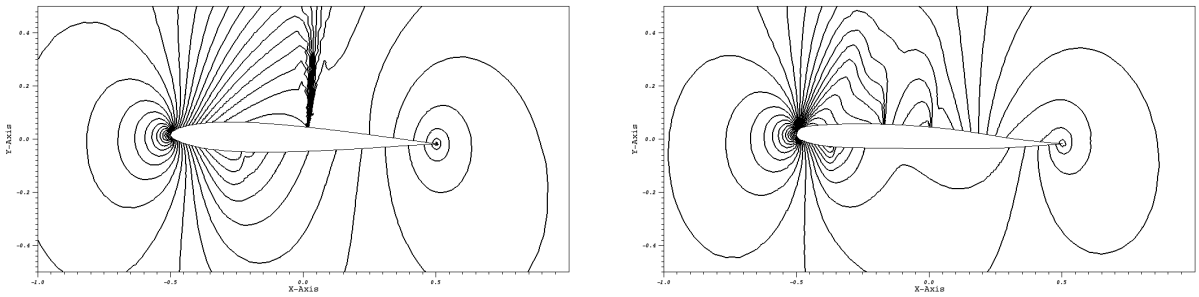

Figure 5: Comparison of pressure fields for the initial airfoil (left) and Nash equilibrium (right).

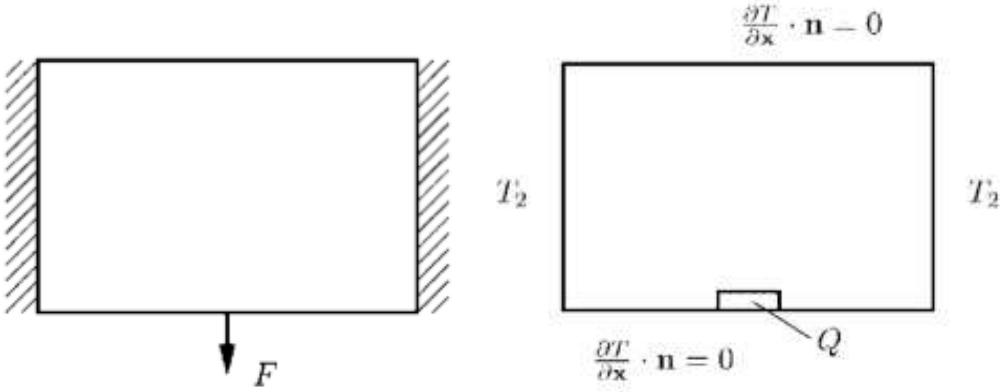

Figure 6: Design domain for player J_A (left) and player J_B (right).

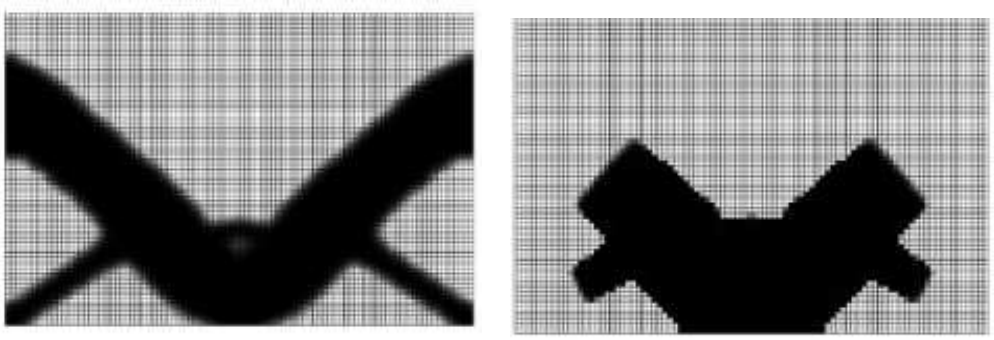

Figure 7: Nash equilibrium topologies for player J_A (left) and player J_B (right).

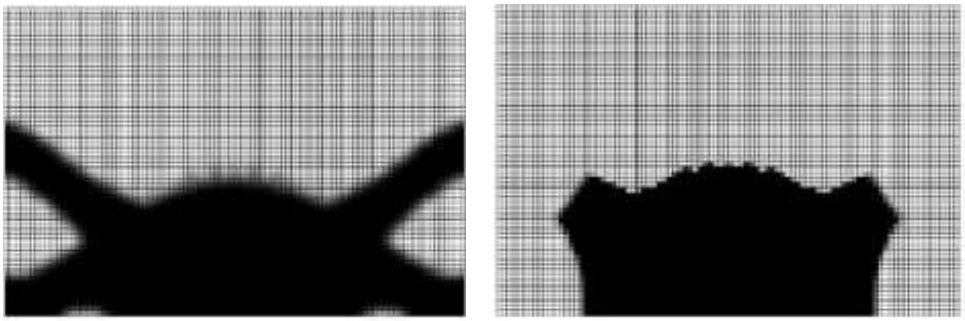

Figure 8: Optimal distribution for ρ_1 and ρ_2 for $\lambda = 0.5$.

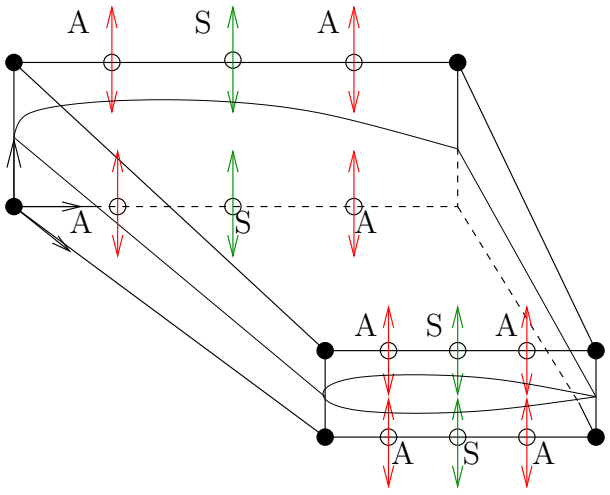

Figure 9: Aero-structural shape optimization of a business jet wing; first split of territory, according to the primitive variables : parameters marked A are associated to aerodynamics, and those marked S to structural design.

a) Drag (J_A) *b) Stress integral (J_S)*

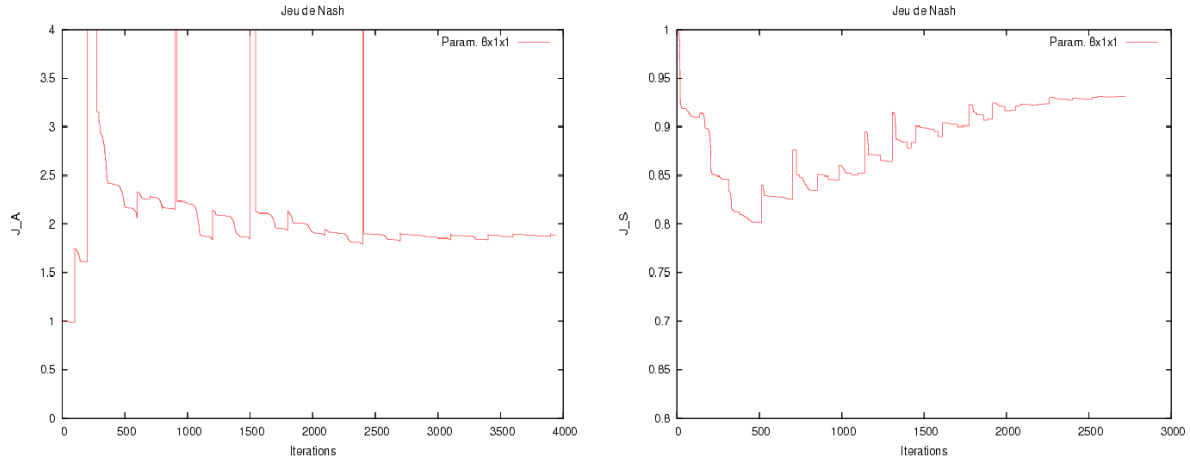

Figure 10: Aero-structural shape optimization of a business jet wing; first split of territory, according to the primitive variables : convergence history of the aerodynamic and structural criteria.

a) Purely aerodynamic optimization *b) Nash equilibrium (unacceptable solution)*

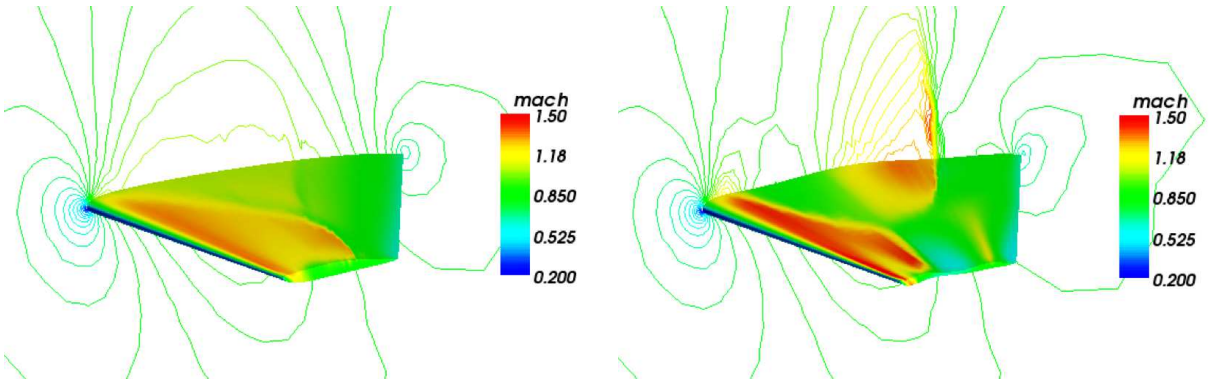

Figure 11: Aero-structural shape optimization of a business jet wing; first split of territory, according to the primitive variables : shape and Mach number field : a) purely aerodynamic optimization, and b) Nash equilibrium.

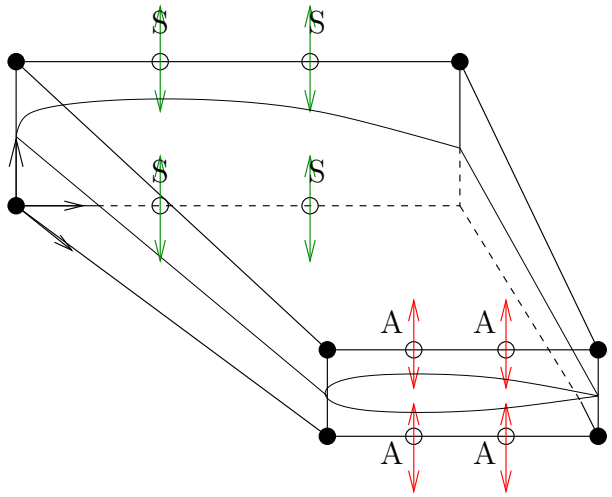

Figure 12: Aero-structural shape optimization of a business jet wing; second split of territory, according to the primitive variables : parameters marked A are associated to aerodynamics, and those marked S to structural design.

a) Convergence history

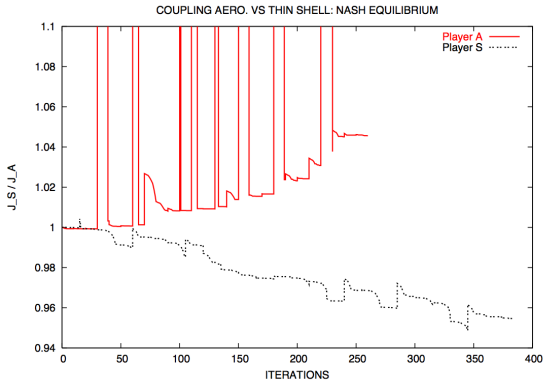

b) Shape at root

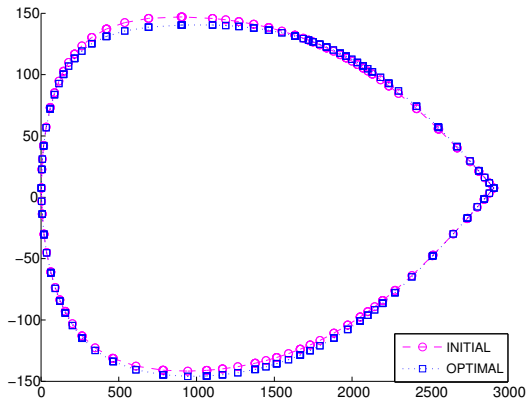

c) Shape at mid-span

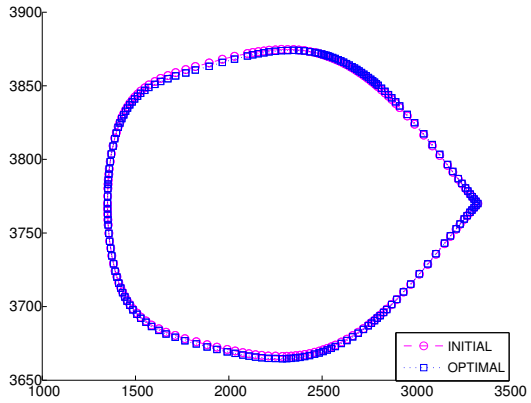

d) Shape at wing tip

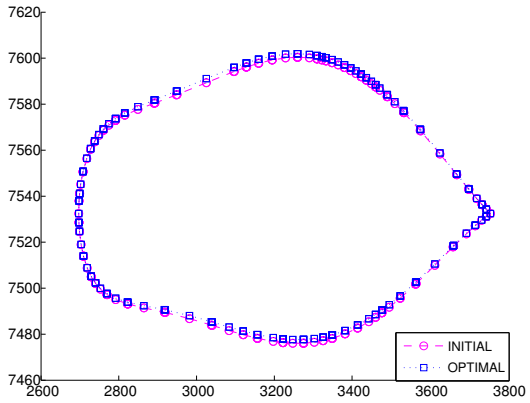

Figure 13: Aero-structural shape optimization of a business jet wing; second split of territory, according to the primitive variables : a) convergence history of the two criteria; b), c) and d) cross-section variations at root, mid-span, and wing tip. (Coordinates are in mm.)

a) Convergence history

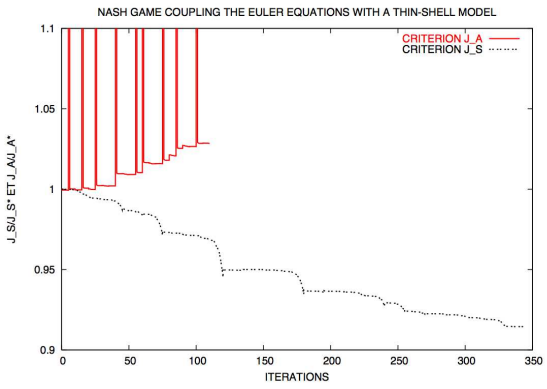

b) Shape at root

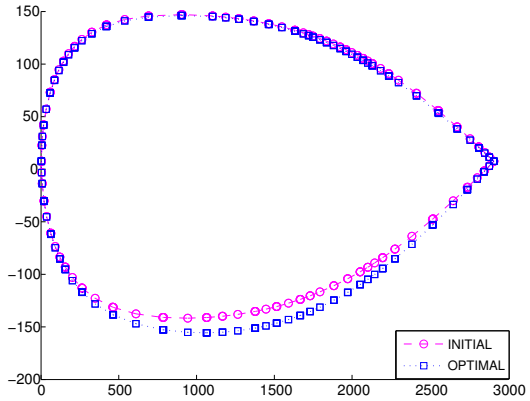

c) Shape at mid-span

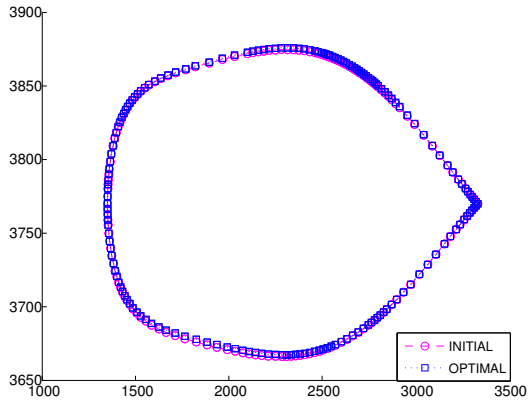

d) Shape at wing tip

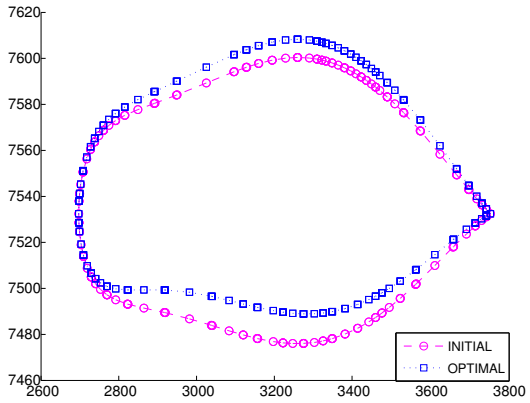

Figure 14: Aero-structural shape optimization of a business jet wing; split of variables according to the orthogonal decomposition : a) convergence history of the two criteria (after 50 couplings); b), c) and d) cross-section variations at root, mid-chord, and wing tip. (Coordinates are in mm.)

a) Initial aerodynamic optimum solution

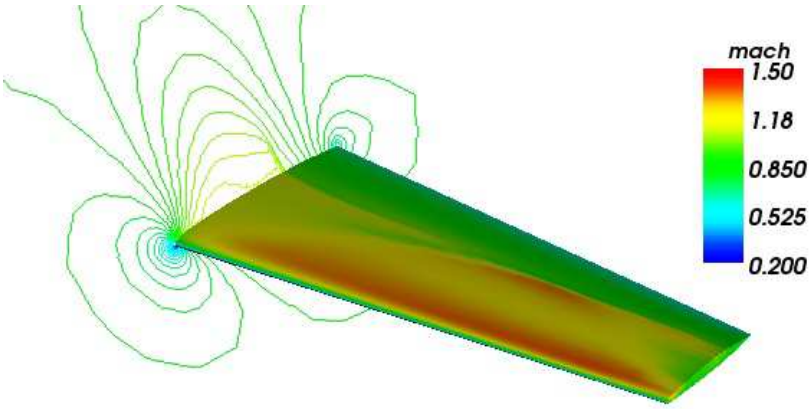

b) Aero-structural Nash game solution using the orthogonal decomposition

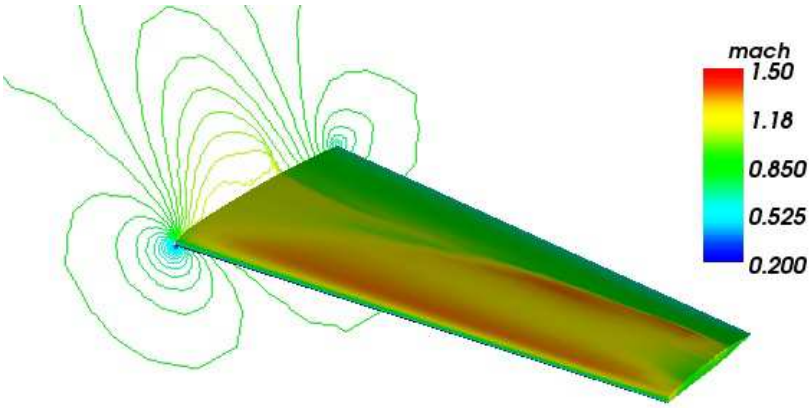

Figure 15: Geometrical configuration and Mach number field : a) initial aerodynamic optimum solution, and b) aero-structural Nash game solution using the orthogonal decomposition.

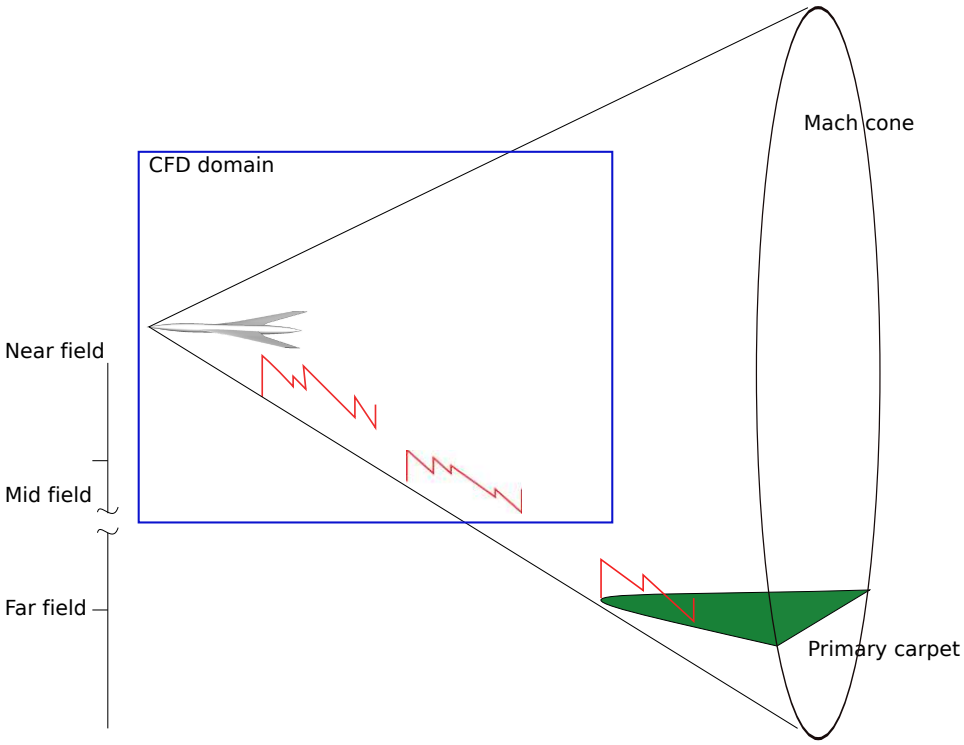

Figure 16: Sonic boom problem configuration. (The scales have been distorted for purpose of sketch: the computational domain extends over 5 body lengths, whereas the far-field primary carpet is located at 18 kms.)

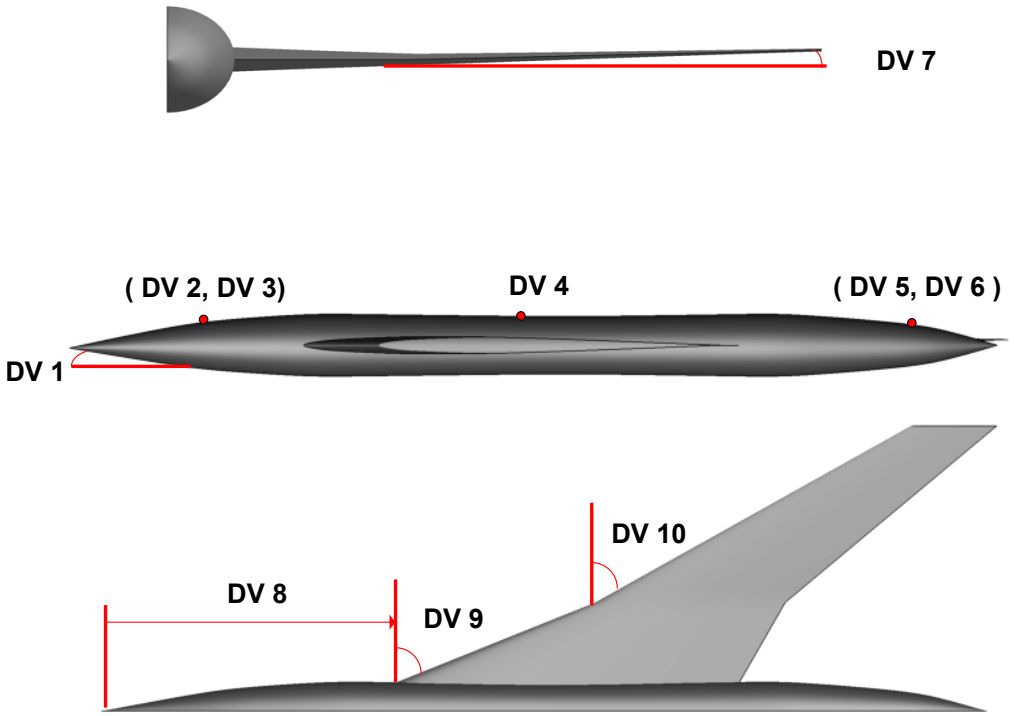

Figure 17: Geometrical design parameters for sonic boom problem. In the optimization by a Nash game, only the following 5 parameters have been retained: DV1, DV3, DV4, DV7 and DV8.

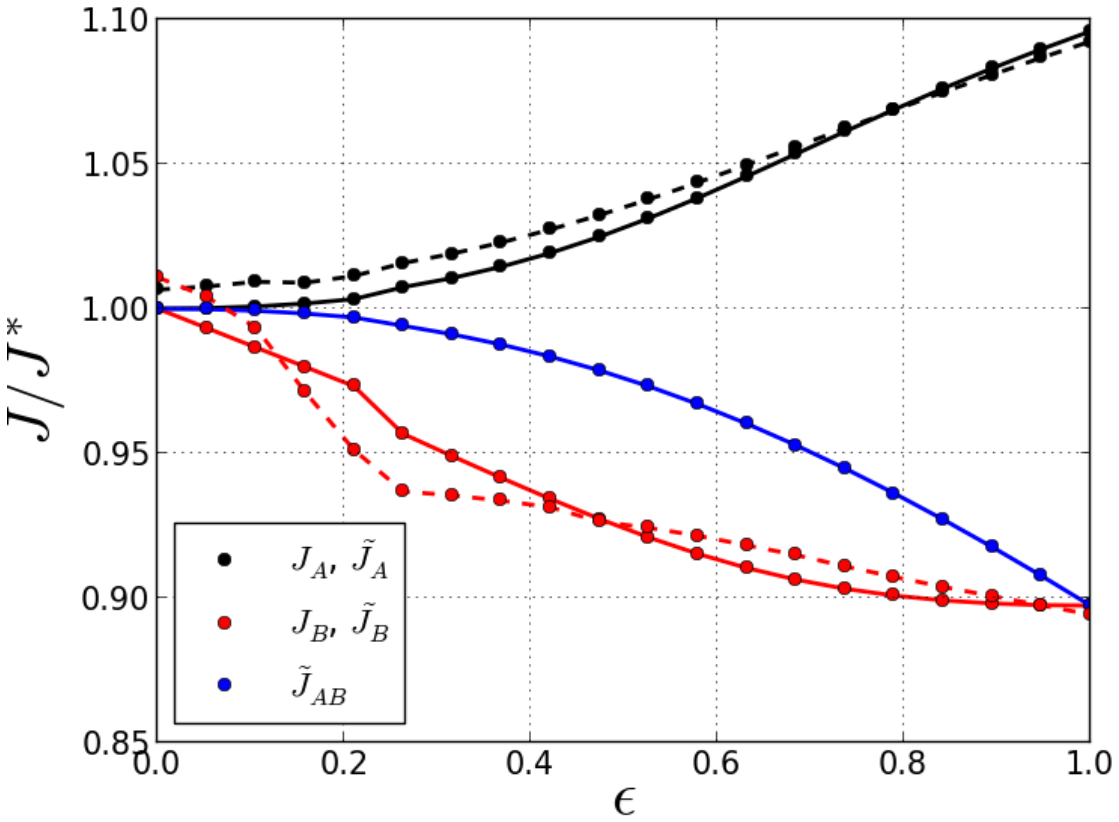

Figure 18: Sonic boom problem. Convergence history of the objective functions as the continuation parameter ϵ is incremented. The ordinate axis indicates for different objective functions J, the ratio $J(\bar{\mathbf{y}}_\epsilon)/J(\mathbf{y}_A^\star)$, where $\mathbf{y}_A^\star$ corresponds to the optimum of $\tilde{J}_A$ under lift meta-model constraint, and $\bar{\mathbf{y}}_\epsilon$ to the Nash-equilibrium design-point. Solid lines are associated with meta-models, and dotted lines with actual CFD *a posteriori* simulations.

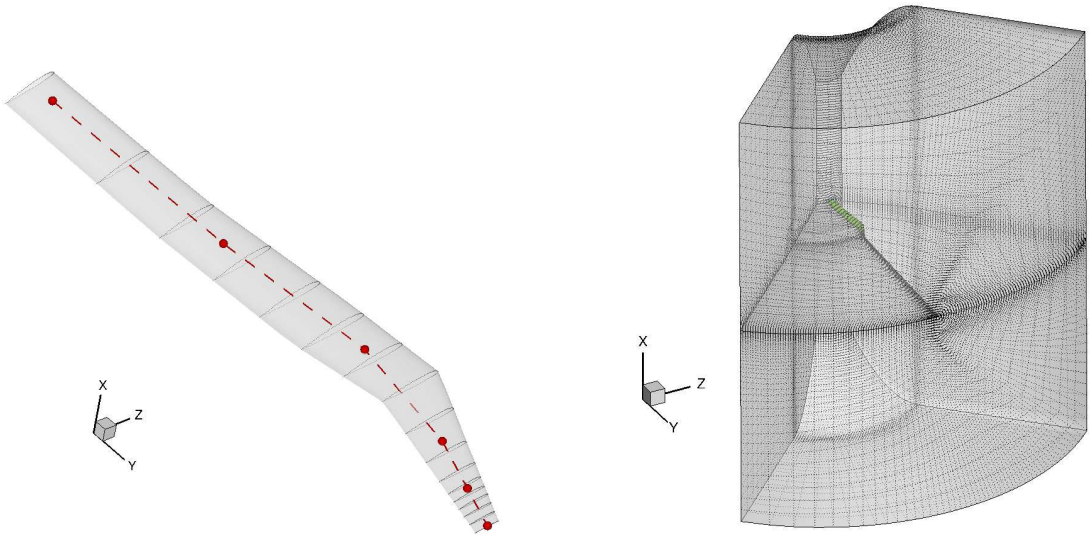

Figure 19: ERATO blade: Bézier poles discretization (left) and 3D mesh (right).

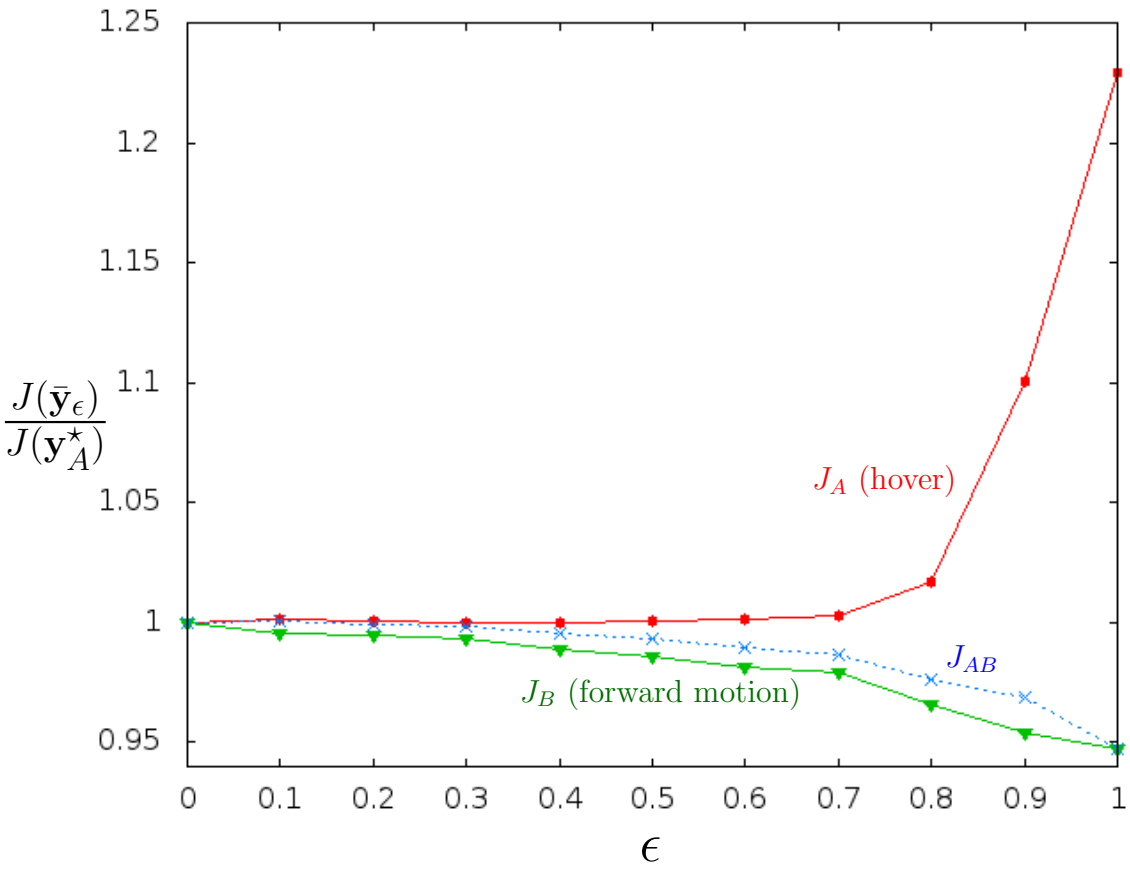

Figure 20: Rotor blade two-point/two-objective optimization. Convergence history of the objective functions as the continuation parameter ϵ is incremented. The ordinate axis indicates the values of the objective functions $J = J_A$, J_{AB}, or J_B evaluated at the Nash equilibrium point $\bar{\mathbf{y}}_\epsilon$ between J_A and J_{AB} at a given ϵ, normalized by the value the criterion at the point $\mathbf{y}_A^\star$ of absolute optimum of J_A alone. J_A is the Figure of Merit in hovering configuration; J_B is the requires power for forward motion.

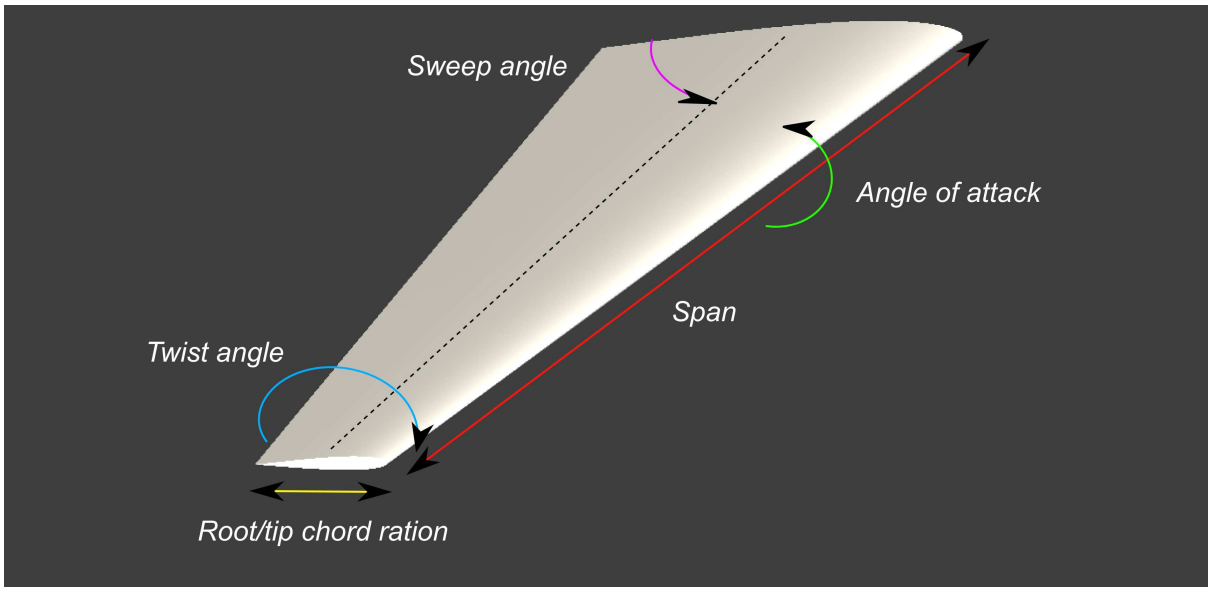

Figure 21: Parameters for global wing characteristics.

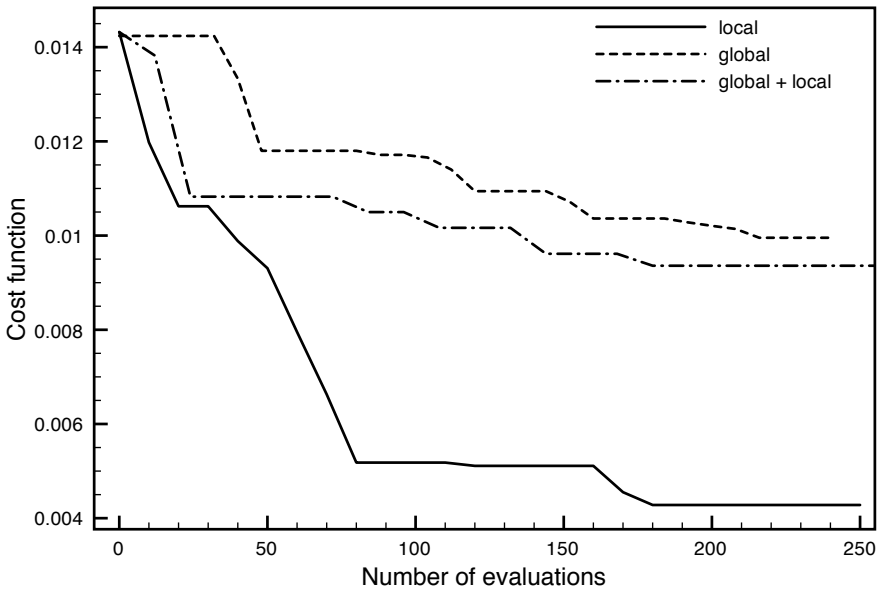

Figure 22: Evolution of the cost function for single optimizations.

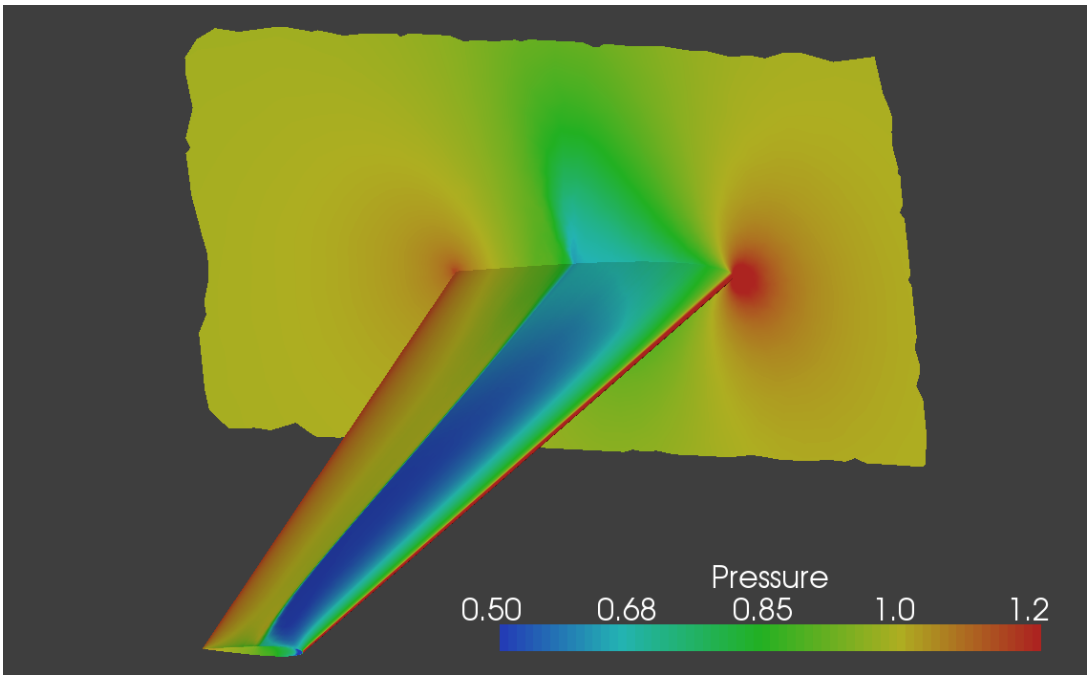

Figure 23: Pressure field for baseline shape.

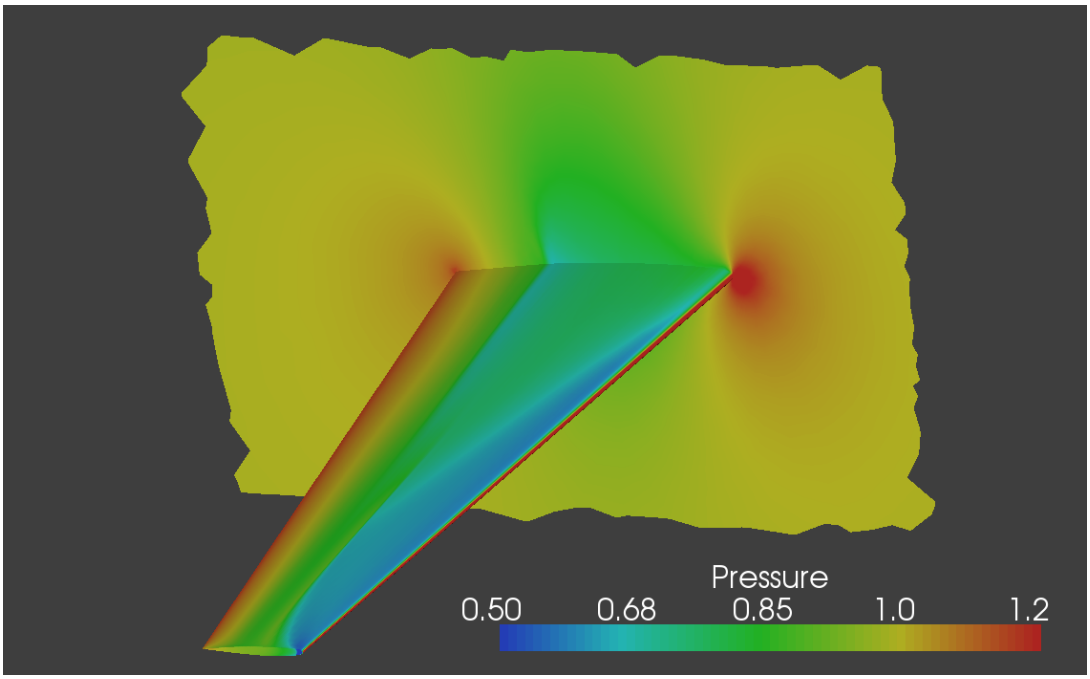

Figure 24: Pressure field for optimized local parameters.

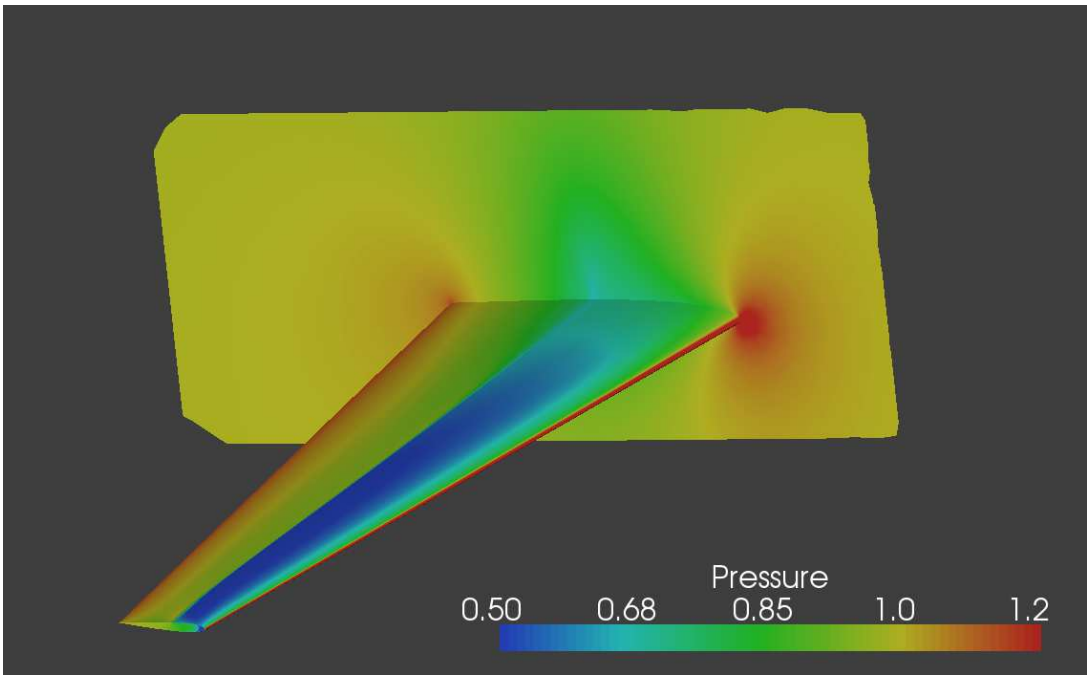

Figure 25: Pressure field for optimized global parameters.

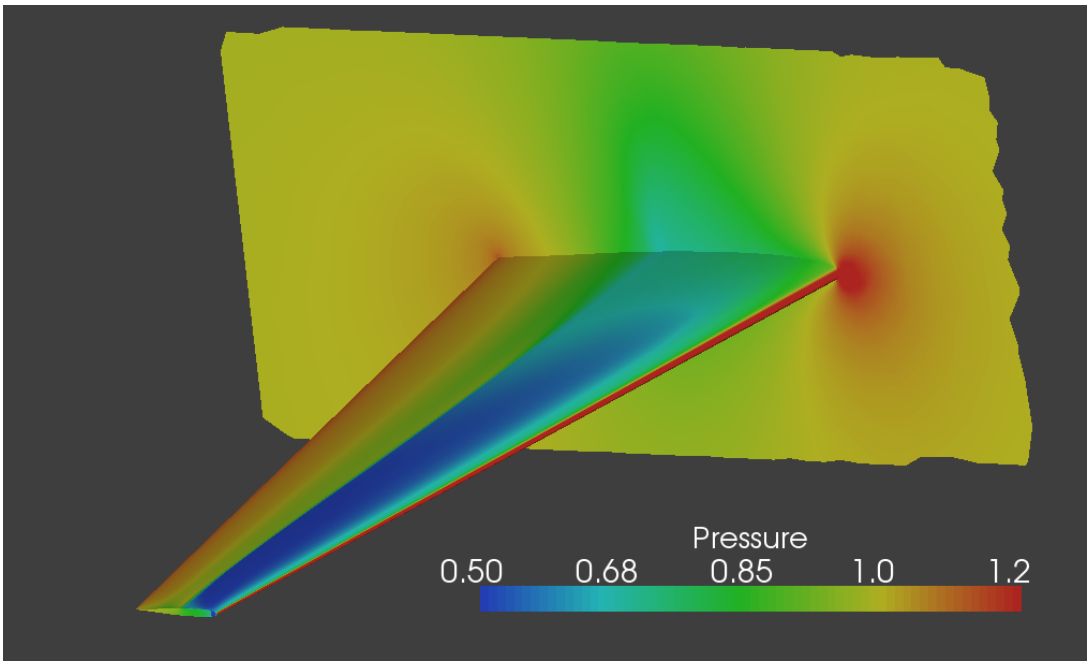

Figure 26: Pressure field for optimized global and local parameters.

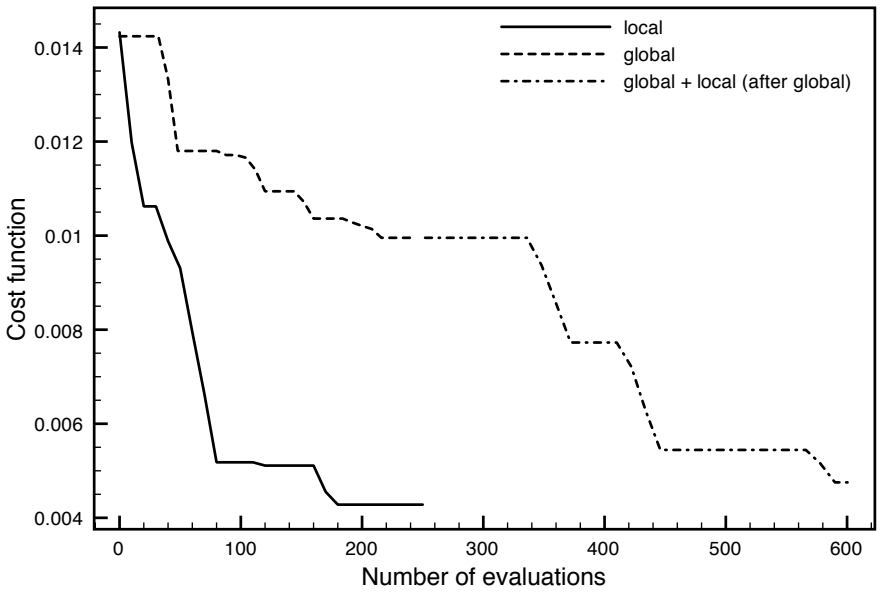

Figure 27: Evolution of the cost function for the nested optimizations.

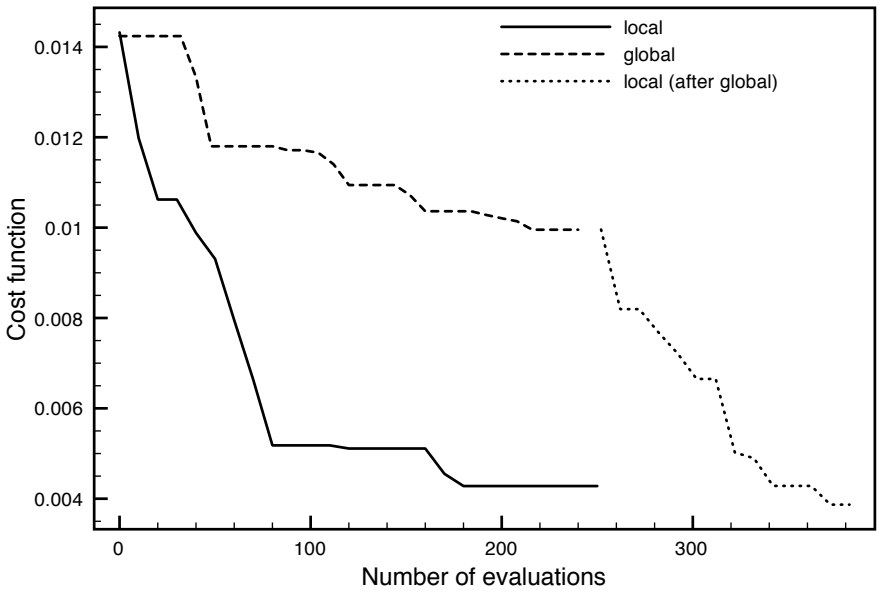

Figure 28: Evolution of the cost function for the successive optimizations approach.

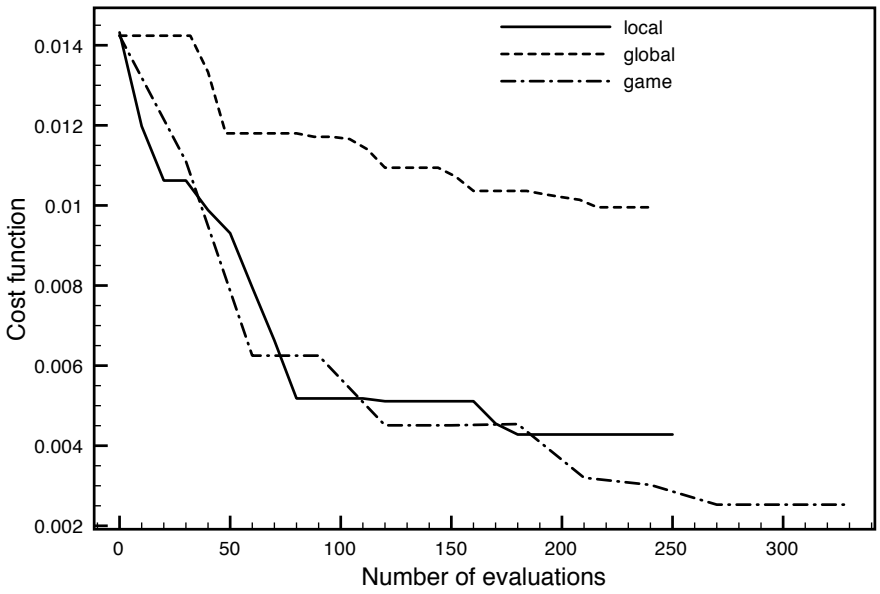

Figure 29: Evolution of the cost function for the game strategy.

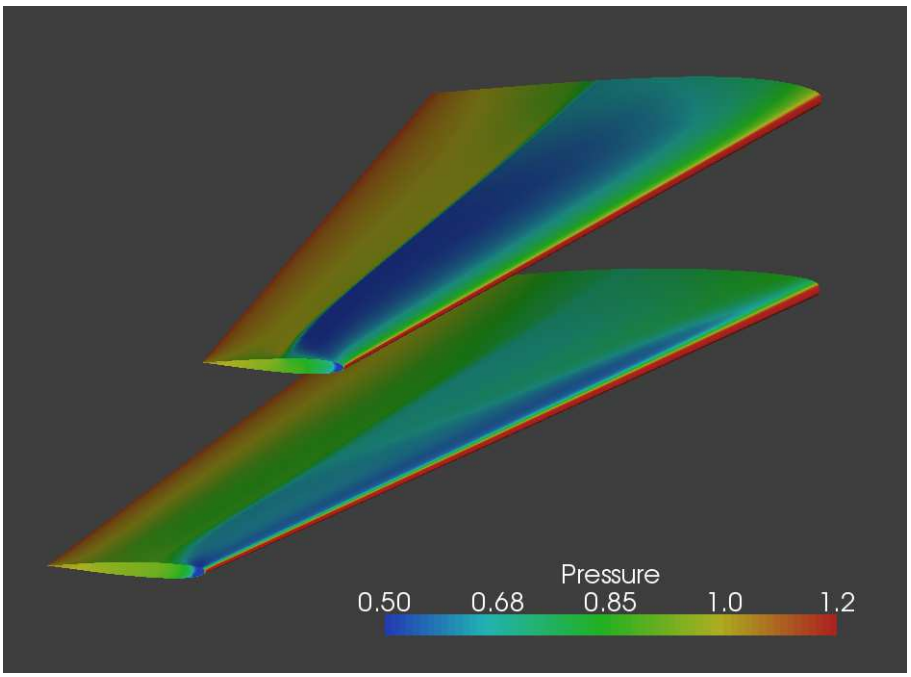

Figure 30: Comparison of the pressure field for the initial wing and the wing optimized by Nash game.